Department of Chemical and Metallurgical Engineering

# Experimental thermodynamic and kinetic studies on extraction and recycling of lead from spent lead-acid battery paste

Yun Li

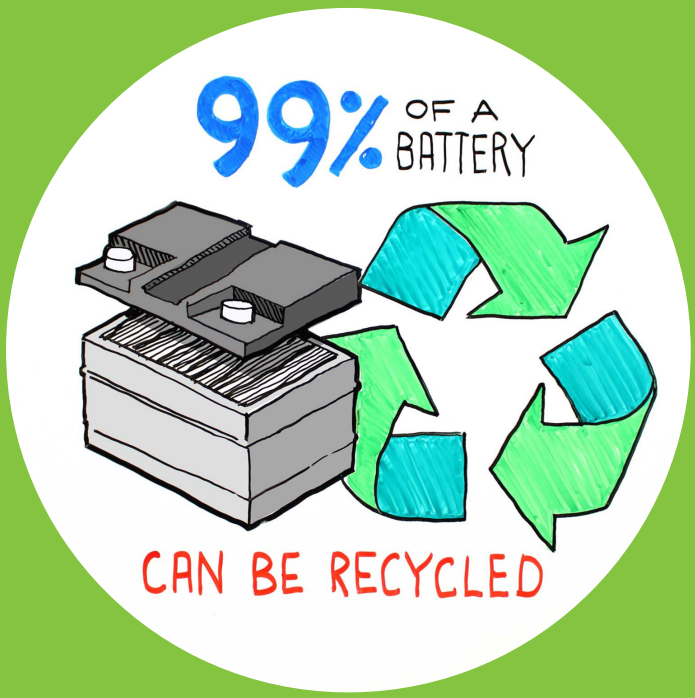


Aalto University

DOCTORAL DISSERTATIONS

Aalto University publication series
**DOCTORAL DISSERTATIONS** 95/2019

# Experimental thermodynamic and kinetic studies on extraction and recycling of lead from spent lead-acid battery paste

**Yun Li**

A doctoral dissertation completed under a well-organized double degree project to be defended, with the permission of the Aalto University School of Chemical Engineering, and with the permission of Central South University. The public examination will be held at Metallurgy Building lecture hall 301, Central South University, Changsha, China, on 28th May 2019 at 15 pm (Chinese time), and an on-line connection to Aalto University will be shown at Ke 5, lecture hall, Kemistintie 1, Espoo, Finland

**Aalto University**
**School of Chemical Engineering**
**Department of Chemical and Metallurgical Engineering**
**Metallurgy**

**Supervising professors**
Professor Shenghai Yang, Central South University, P.R. China
Professor Ari Jokilaakso, Aalto University, Finland

**Thesis advisors**
Professor Yongming Chen, Central South University, P.R. China
Professor Emeritus Pekka Taskinen, Aalto University, Finland

**Preliminary examiners**
Professor Ing. Andrea Miškufová, Technical University of Košice, Slovakia
Professor Timo Fabritius, University of Oulu, Finland
Professor Jianguang Yang, Central South University, P.R. China

**Opponents**
Professor Yongxiang Yang, Delft University of Technology (TU Delft), the Netherlands
Professor Zhihong Liu, Central South University, P.R. China
Professor Tianzu Yang, Central South University, P.R. China
Professor Daniel Lindberg, Aalto University, Finland.
Professor Xiaoyuan Zhou, Changsha Institute of Nonferrous (CINF) Engineering Corporation Limited, P.R. China

Aalto University publication series
**DOCTORAL DISSERTATIONS** 95/2019



ISBN 978-952-60-8561-6 (printed)
ISBN 978-952-60-8562-3 (pdf)
ISSN 1799-4934 (printed)
ISSN 1799-4942 (pdf)
http://urn.fi/URN:ISBN:978-952-60-8562-3

Unigrafia Oy
Helsinki 2019

Finland

NORDIC SWAN ECOLABEL
Printed matter
4041-0619

Aalto University

# Abstract

Aalto University, P.O. Box 11000, FI-00076 Aalto www.aalto.fi

**Author**
Yun Li

**Name of the doctoral dissertation**
Experimental thermodynamic and kinetic studies on extraction and recycling of lead from spent lead-acid battery paste

**Publisher** School of Chemical Engineering

**Unit** Department of Chemical and Metallurgical Engineering

**Series** Aalto University publication series DOCTORAL DISSERTATIONS 95/2019

**Field of research** Processing of Materials

**Manuscript submitted** 29 April 2019 **Date of the defence** 28 May 2019

**Permission for public defence granted (date)** 25 April 2019 **Language** English

☐ **Monograph** ☒ **Article dissertation** ☐ **Essay dissertation**

**Abstract**

Lead recycling from complex secondary materials has gained increasing interest in recent years. Around 80-85% of the total secondary lead is recycled from lead paste. Due to the high toxicity of lead and increasingly stringent environmental regulations, cleaner and efficient processing of such materials and development of industrial processes are urgently required.

In the present work, an innovative and clean lead-acid battery paste recycling technique is proposed. Iron-containing waste materials are utilized as sulfur-fixing agents to capture sulfur as FeS, instead of generating excessive amount of $SO_2$. $Na_2CO_3$ or $Na_2CO_3$-$Na_2SO_4$ salt mixture is added to the smelting system to promote the reactions and improve valuable metals' recovery and sulfur-fixation efficiency.

Thermodynamic calculations and experimental determination of the reaction mechanisms in the $PbSO_4$-$Fe_2O_3$-C, $PbSO_4$-$Na_2CO_3$-C, and $PbSO_4$-$Fe_2O_3$-$Na_2CO_3$-C systems are carried out to build the fundamental knowledge. Thermogravimetric analysis and quenching method coupled with a direct spectroscopic analysis of the phase and chemical compositions of the resulting phases, i.e. XRD and SEM-EDS, are employed to investigate the phase transformation mechanism. The results indicate that without $Na_2CO_3$ addition, lead in lead paste is shown to be extracted mainly through the sequence of $PbSO_4 \xrightarrow{C/CO} PbS \xrightarrow{Fe_3O_4} PbO \xrightarrow{C/CO} Pb$. Sulfur in $PbSO_4$ is thus first transferred to PbS and finally fixed as FeS. In the presence of $Na_2CO_3$, at low temperatures and in weakly reductive atmospheres, lead is extracted mainly through the sequence of $PbSO_4 \xrightarrow{Na_2CO_3} PbO \xrightarrow{C/CO} Pb$. $Na_2CO_3$ helps to transform $SO_3$ from $PbSO_4$ to $Na_2SO_4$. At high temperatures and strong reducing atmospheres, $PbSO_4 \xrightarrow{C/CO} PbS$ dominates the reactions, and lead and sulfur are conserved as PbS. Lead can not be effectively extracted from PbS without a sulfur-fixing agent. When $Fe_2O_3$ is presented, lead in PbS will further be extracted through the sequence of $PbS \xrightarrow{Fe_3O_4} PbO \xrightarrow{C/CO} Pb$. Finally, sulfur is fixed as FeS, $NaFeS_2$ and $Na_2S$.

A series of bench-scale experiments are conducted to detect the influence mechanisms of smelting conditions on lead extraction and sulfur fixation efficiency. The optimum smelting parameters obtained are integrated to an industrial pilot campaign. Under the optimum conditions, three smelting products, crude lead, ferrous matte, and slag, are formed. 91%-96% lead in the initial raw materials is found to be enriched in crude lead bullion. 97%-99% sulfur is fixed in the sulfide matte and slag. Purity of the crude lead reaches 96%-98%. Lead concentrations in the matte and slag are below 2.4%-4.1% and 0.5-1.2%, respectively, without subsequent matte and slag cleaning. The addition of sodium salts, e.g. $Na_2CO_3$ and a $Na_2CO_3$-$Na_2SO_4$ mixture, is seen to promote the reductive sulfur-fixing reactions and improve extraction and sulfur-fixation efficiency.

**Keywords** Lead-acid battery paste, lead recycling, $SO_2$-free sulfur-fixing smelting, waste co-treatment and recycling, lead-iron containing wastes, phase diagram

**ISBN (printed)** 978-952-60-8561-6 **ISBN (pdf)** 978-952-60-8562-3

**ISSN (printed)** 1799-4934 **ISSN (pdf)** 1799-4942

**Location of publisher** Helsinki **Location of printing** Helsinki **Year** 2019

**Pages** 123 **urn** http://urn.fi/URN:ISBN:978-952-60-8562-3

# Preface

The author was studying for the doctoral degree at the period of September 2015---2019. This doctoral thesis work was conducted under a well-organized double-degree project between Central South University (CSU, School of Metallurgy and Environment) and Aalto University (Aalto, School of Chemical Engineering). The research presented in this thesis was carried out in both universities, Metallurgy (MTG) research group in Aalto and School of Metallurgy and Environment in CSU.

I would like to express my deepest acknowledgement to my supervisors, Professor Ari Jokilaakso from Aalto and Professor Shenghai Yang, Professor Yongming Chen, and Professor Chaobo Tang from CSU. Thanks for giving me the valuable opportunity to study pyrometallurgy and thermodynamic in two high reputation universities. I appreciate your amazing guidance, support, and the freedom and space you have offered to me during this study. Likewise, I thank Professor Pekka Taskinen, my thesis advisor, for helping me to muster professional thermodynamic skills and knowledge. Thank you for reviewing and commenting my manuscripts in many early morning and even weekends. The considerable help from you will be memorized forever.

All the input from the pre-examiners, Professor Ing. Andrea Miškufová from Technical University of Košice, Professor Timo Fabritius from University of Oulu, Professor Tianzu Yang and Professor Jianguang Yang from Central South University, are very important in improving the quality of this present thesis. The author is grateful to your wonderful work.

This thesis work was financially suppported by Aalto University School of Chemical Engineering. I acknowledge the financial support for materials characterization with the Academy of Finland's RawMatTERS Finland Infrastructure (RAMI) based at Aalto University.

I wish to thank Professor Zhihong Liu, Professor Longgong Xia, Professor Xiaobo Min and Professor Tiangui Qi from CSU side, and Professor Daniel Lindberg, Ms. Sirje Liukko from Aalto side, for warmly helping me on my double-degree project application. Without your kind work, I can never fulfil my dream.

My MTG colleagues in Aalto, Dr. Dmitry Sukhomlinov, M.Sc. Lassi Klemettinen, M.Sc. Minna Rämä, Dr. Niko Hellstén, M.Sc. Xingbang Wan, Dr. Imam Santoso, Dr. Junjie Shi, Dr. Min-kyu Paek are acknowledged for your help and support, assistance in experiments and analysis and just for being great work-

mates. My friends in Finland and China with whom I had pleasure to accompany during my doctoral study period are thanked.

My deepest gratitude goes to my parents, wife and lovely son for trust, inspiration and encouragement. You are my most important motivation resources during the past years.

Kemistintie 1 F, Espoo
18 February 2019
Yun Li

# Contents


Preface ..... 1
List of abbreviations and symbols ..... 5
List of publications ..... 7
Author's contribution ..... 8
1. Introduction ..... 10
1.1 Research background ..... 10
1.2 Objectives and scope ..... 12
1.3 New scientific contribution ..... 13
1.4 Research approach and process ..... 13
1.5 Practical application ..... 14
1.6 Structure of the thesis ..... 15
2. Experimental ..... 17
2.1 Materials ..... 17
2.2 Equipment ..... 18
2.3 Methods ..... 19
2.3.1 Experimental procedure ..... 19
2.3.2 Analytical methods ..... 20
2.3.3 Calculation of the yields ..... 21
3. Results and discussion ..... 22
3.1 Thermodynamic calculation of RSFS process ..... 22
3.1.1 Main reactions and Gibbs energy change ..... 22
3.1.2 Equilibrium compositions ..... 23
3.1.3 Phase diagrams ..... 24
3.2 The phase conversion mechanisms and kinetics ..... 25
3.2.1 $PbSO_4$-$Fe_2O_3$-C system ..... 25
3.2.2 $PbSO_4$-$Na_2CO_3$-C system ..... 27
3.2.3 $PbSO_4$-$Fe_2O_3$-$Na_2CO_3$-C system ..... 28
3.3 Lead paste recycling with sulfur fixation using hematite ..... 31
3.4 Lead paste recycling and sulfur fixation with $Na_2CO_3$ ..... 35

3.4.1 Hematite ..... 35
3.4.2 Jarosite residue ..... 37
3.5 Complex Pb-containing wastes recycling in $Na_2CO_3$-$Na_2SO_4$ .39
3.6 Industrial pilot trial and environmental evaluation..... 41
4. Conclusions ..... 44
References ..... 46

# List of abbreviations and symbols

**Abbreviations**

| | |
|---|---|
| LAB | Lead-acid battery |
| CRT | Cathode ray tubes |
| PyC | Pyrite cinder |
| JaR | Jarosite residue |
| LR | Leaching residue |
| RSFS | Reductive sulfur-fixing smelting |
| SFA | Sulfur-fixing agent |
| XRD | X-ray diffractometer |
| SEM | Scanning electron microscope |
| EDS | Energy dispersive spectroscopy |
| TG-DTA | Thermogravimetric analysis |
| ICP-AES | Inductively coupled plasma-atomic emission spectrometry |
| OPEX | Operating expenditure |

**Symbols**

| | |
|---|---|
| $\eta$ | Direct Pb recovery |
| $\gamma$ | Sulfur-fixing rate |
| $\Delta G_T^\theta$ | Gibbs free energy change |
| kJ | Kilojoule |
| T | Temperature |
| t | Time |
| d | Day |
| h | Hour |
| min | Minute |

| | |
|---|---|
| ml/min | Millilitres per minute |
| n | Mole |
| W | Weight ratio |
| wt% | Weight fraction |
| °C | Centigrade degree |
| K | Kelvin |
| mg | Milligram |
| Mpa | Mega Pascal |

# List of publications

This doctoral dissertation consists of a summary and of the following publications which are referred to in the text by their respective numerals.

**I.** Yun Li, Shenghai Yang, Pekka Taskinen, Jing He, Fangwen Liao, Rongbo Zhu, Yongming Chen, Chaobo Tang, Yuejun Wang, Ari Jokilaakso. 2019. Novel recycling process for lead-acid battery paste without $SO_2$ generation - Reaction mechanism and industrial pilot campaign. Elsevier. Journal of Cleaner Production, volume 217, Pages 162-171. ISSN: 0959-6526. DOI: 10.1016/j.jclepro.2019.01.197.

**II.** Yun Li, Shenghai Yang, Pekka Taskinen, Jing He, Yongming Chen, Chaobo Tang, Yuejun Wang, Ari Jokilaakso. Spent lead-acid battery recycling via reductive sulfur-fixing smelting and its reaction mechanism in the $PbSO_4$-$Fe_3O_4$-$Na_2CO_3$-C system. Springer. ISSN: 1543-1851. DOI: 10.1007/s11837-019-03518-4 (Accepted)

**III.** Yun Li, Shenghai Yang, Wenrong Lin, Pekka Taskinen, Jing He, Yuejun Wang, Junjie Shi, Yongming Chen, Chaobo Tang and Ari Jokilaakso. 2019. Cleaner Extraction of Lead from Complex Lead-Containing Wastes by Reductive Sulfur-Fixing Smelting with Low $SO_2$ Emission. MDPI. Minerals, volume 9, Issue 2, Ar_cle number: 119. ISSN: 2075-163X. DOI: 10.3390/min9020119

**IV.** Yun Li, Shenghai Yang, Pekka Taskinen, Jing He, Chaobo Tang, Yongming Chen, Yuejun Wang, Ari Jokilaakso. Cleaner recycling of spent lead-acid battery paste and harmless treatment of pyrite cinder via reductive sulfur-fixing method for valuable metals recovery. Submit to Resources, Conservation and Recycling in 2019.

# Author's contribution

**Publication I:** Novel recycling process for lead-acid battery paste without $SO_2$ generation - Reaction mechanism and industrial pilot campaign

The author organized the research plan, conducted experimental work, wrote and modified the manuscript according to Prof. Ari Jokilaakso's and Prof. Pekka Taskinen's comments; Prof. Shenghai Yang performed the supervising work; Prof. Ari Jokilaakso reviewed the results and conclusion; Prof. Pekka Taskinen critically reviewed the thermodynamic work and checked the English language; Prof. Jing He assisted with data interpretation; Fangwen Liao and Rongbo Zhu assisted with the sample preparation for ICP-AES and XRD analysis. Prof. Yongming Chen, Prof. Chaobo Tang and Prof. Yuejun Wang were in charge of the project administration.

**Publication II:** Spent lead-acid battery recycling via reductive sulfur-fixing smelting and its reaction mechanism in the $PbSO_4$-$Fe_3O_4$-$Na_2CO_3$-C system

The author defined the research plan, carried out all the experiments and data analysis, wrote, revised and submitted the manuscript; Prof. Shenghai Yang and Prof. Ari Jokilaakso performed the supervising work; Prof. Pekka Taskinen calculated the phase diagram and reviewed the manuscript; Prof. Jing He assisted with data interpretation; Prof. Yongming Chen, Prof. Chaobo Tang and Prof. Yuejun Wang contributed the project administration.

**Publication III:** Cleaner Extraction of Lead from Complex Lead-Containing Wastes by Reductive Sulfur-Fixing Smelting with Low $SO_2$ Emission

The author conducted the experimental works, data collection and analysis, wrote and modified the manuscript based on Prof. Ari Jokilaakso's and Prof. Pekka Taskinen's comments; Prof. Shenghai Yang performed the supervising work; Wenrong Lin assisted the experimental work and sample analysis; Prof. Jing He and Prof. Yuejun Wang assisted the design of the work; Junjie Shi assisted with the data analysis. Prof. Yongming Chen and Prof. Chaobo Tang were in charge of project administration; Prof. Ari Jokilaakso and Prof. Pekka Taskinen critically reviewed the results and conclusion.

**Publication IV:** Cleaner recycling of spent lead-acid battery paste and harmless treatment of pyrite cinder via reductive sulfur-fixing method for valuable metals recovery

The author organised the research plan, performed the experiments, wrote and revised the manuscript according to the comments from the supervisors and co-authors. Prof. Shenghai Yang, Prof. Yongming Chen and Prof. Chaobo Tang were in charge of project administration and assisted with the supervising work; Prof. Jing He and Prof. Yuejun Wang assisted with the design of research plan; Prof. Ari Jokilaakso and Prof. Pekka Taskinen reviewed and checked the language of the manuscript.

# 1. Introduction

Lead-acid batteries (LABs) are increasingly scrapped in urban areas, especially in the emerging economies, due to their mean lifetime of 2–3 years. LABs are classified as hazardous materials in many countries and their disposal has become a significant environmental concern. Pyrometallugy currently dominates the lead recycling industry worldwide. However, due to the depleting primary resources and increasingly stringent environmental requirements, lead recycling industry is currently under pressure to develop more sustainable processes to achieve new standards of production and emissions. Consequently, researching novel and environment-friendly waste recycling techniques to increase knowledge and enable process optimization for lower environmental impact is mandatory for the modern technology-based society.

## 1.1 Research background

LABs are widely applied in automobile and electric bicycle industries. Recent advances in energy [1], transportation and telecommunication industries [2] have significantly increased the demand and consequent scrap volume growth of LABs worldwide [3, 4]. It is estimated that the amount of spent LABs would multiply annually, based on the mean lifetime of 2–3 years, and will continue to grow [5, 6] especially in China [3, 7-10] and other emerging economies [11]. As a result, LABs have become the most significant secondary lead source worldwide [10, 12-15]. Typically, a spent LAB consists of four components: lead paste (30-40%), lead alloy grids (24-30%), polymeric materials (22-30%), and waste electrolyte (11-30%) [7, 16, 17]. Of these, lead paste is the most difficult part to deal with [18]. It is a mixture of 50-60% $PbSO_4$, 15-35% $PbO_2$, 5-10% $PbO/Pb(OH)_2$, 2-5% metallic Pb and a small amount of impurities [12, 19], such as iron, antimony, tin and barium. In addition to LABs, more and more interest is also being expressed in recycling lead from other complex lead-containing secondary materials [20-25], including lead sludge, cathode ray tubes (CRT) [26], lead dusts and slags produced in various lead metallurgical processes.

The destiny of spent LABs is of great environmental concern [27, 28], due to the high toxicity of lead [29, 30]. If treated improperly [31], lead waste would be a serious threat to environmental safety [32-34] and human health [4, 6, 35]. Currently, scrap LAB recycling technology [4] primarily includes pyrometallurgy and hydrometallurgy [36, 37]. In the hydrometallurgical process

[38-40], a pre-desulfurization procedure [19, 41] is necessary. $Na_2CO_3$, NaOH, $K_2CO_3$ solutions or citric acid and citrate salts are usually adopted as desulfuration reagents [42]. Hydrometallurgy is usually considered as low cost and green technology, however, some environmental problems resulting from emission of various poisonous gases, such as HCl, $H_2S$ and $AsH_3$ during the processing, still exist and need to be solved [43].

Pyrometallurgy [44, 45] is globally the predominant methodology at present for spent LAB recycling. Reverberatory furnaces, shaft furnaces, electric furnaces, rotary furnaces [46] and bottom blowing method [47] are usually selected to smelt lead-containing residues and wastes [44], including lead paste, lead dust, various leaching residues produced from zinc hydrometallurgy. Although BAT (Best Available Techniques) for spent LABs recycling is suggested by European Commission [48], serious pollution from spent LABs is still possible [11], for e.g. due to lead particulates, discharge of toxic and unstable sludge, slag, and wastewater [49]. Furthermore, the industrial $SO_2$ pollution [33] situation remains grim since sulfur-bearing materials typically are treated in oxidizing atmosphere to remove sulfur as gaseous $SO_2$ [50]. Thus, the emissions of $SO_2$ [44, 51] are common, especially in metallurgical industry.

Some emerging technologies [28, 37, 44, 52], including electrowinning [53], solid phase electrolysis [54], biological technique [55, 56], and vacuum methods [18, 57, 58] etc., are being developed and applied. However, in most methods some problems still exist and need to be solved, e.g. sulfur removing and footprint, lead-containing dust and $SO_2$ emission in pyrometallurgy; tedious procedures, large amount of unmanageable waste water generation and high electricity consumption [4] in hydrometallurgy. A cleaner and more efficient lead recycling technology is therefore needed for handling the growing amount of lead-containing secondary raw materials [59-61].

Furthermore, iron-containing waste materials and residues, including JaR produced from zinc hydrometallurgy [62, 63], and pyrite cinder (PyC) [64, 65] generated in sulfuric acid manufacture, blast furnace bag filter dust [66], and various iron sludges, are produced in large quantities in many industrial processes. They often contain toxic metals including Pb, Cd, As etc., as well as appreciable quantities of valuable metals, such as Cu, Co, In, Au, and Ag [65]. The recycling or harmless treatment of these materials is a challenge [67]. Large quantities of such waste materials are simply landfilled or dumped on land without any treatment [64]. This leads to serious consequences, such as occupation of considerable land resources, dust problems, contamination of soil and underground water [65].

Reductive sulfur-fixing smelting (RSFS) [45, 68, 69] is a novel pyrometallurgical recycling technique. The basic process flowchart for lead-containing secondary materials recycling by RSFS is shown in Figure 1. This novel technique is distinguished from conventional pyrometallurgy techniques like oxidized matte smelting and reductive smelting, by a reductive processing atmosphere and at the same time combined with sulfur transformation and fixation as a sulfide matte. The smelting products obtained contain three solidified products namely, crude metal bullion, matte and slag.

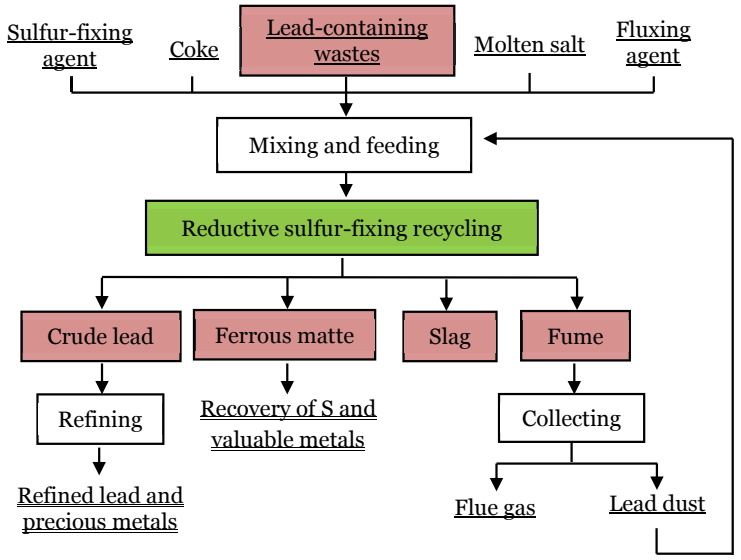


**Figure 1.** Flowchart of reductive sulfur-fixing smelting process for lead extraction and sulfur fixation.

In the RSFS process, the major metals and precious metals, including Au, Ag, Pt, and Pd etc., are enriched in the crude metal bullion; sulfur in the raw materials is transformed and fixed as sulfide matte with the help of the added sulfur-fixing agent (SFA); and finally, the gangue and impurities form a slag. The SFAs generally are selected from the secondary oxide materials or wastes and residues.

## 1.2 Objectives and scope

In view of the stringent environmental regulations, treatment costs and limited availability of landfill/disposal sites, the search for new and cost effective practices for the recycling of LABs and valorization of iron-containing wastes and residues has become increasingly important in recent years [29]. The objectives of this thesis are:

1) To propose a novel integrated recycling treatment method to recover lead, iron and sulfur values without excessive $SO_2$ emissions and co-treat wastes and residues.
2) To examine the thermodynamic feasibility and calculate the equilibrium compositions of the method.
3) To experimentally study the phase conversion mechanisms and reaction paths in the recycling system.
4) To experimentally investigate the feasibility and reliability of this novel process for LAB paste recycling.
5) To reveal the influence mechanisms of different smelting conditions on lead extraction yield and sulfur fixation efficiency.
6) To investigate and determine the optimum conditions for efficient lead and sulfur recovery.

7) To integrate optimized RSFS technique package and conduct an industrial pilot trial.
8) To expand the application of this smelting process to recycle and co-treat various and complex lead-, iron-, zinc-, copper-, antimony-, and bismuth-containing secondary materials.

## 1.3 New scientific contribution

Thermogravimetric analysis (TG-DTA) combined with thermodynamic calculation and experimental phase transformation path investigations of synthetic system were adopted to examine and summarize reaction mechanisms in a complex reaction system. At the same time, the stage primary-phase quenching method coupled with phase composition analysis XRD and SEM-EDS was used in experimental investigation of synthetic system to study high temperature metallurgical process. The phase transformation mechanisms in the $PbSO_4$-$Fe_2O_3$-C, $PbSO_4$-$Na_2CO_3$-C, and $PbSO_4$-$Fe_2O_3$-$Na_2CO_3$-C systems were obtained.

A novel and environment-friendly lead recycling technique, based on RSFS, was thermodynamically and experimentally proved feasible. The industrial pilot trial results provided a demonstration reference with low-cost, low dust generation, absence of harmful by-product, high production capacity, high efficiency, and a much shorter flowsheet, for various secondary wastes and residues recycling.

## 1.4 Research approach and process

In order to develop and industrially integrate the RSFS technique, thermodynamic software calculations and experimental approaches were combined in this study. The flowsheet of the study is shown in Figure 2.

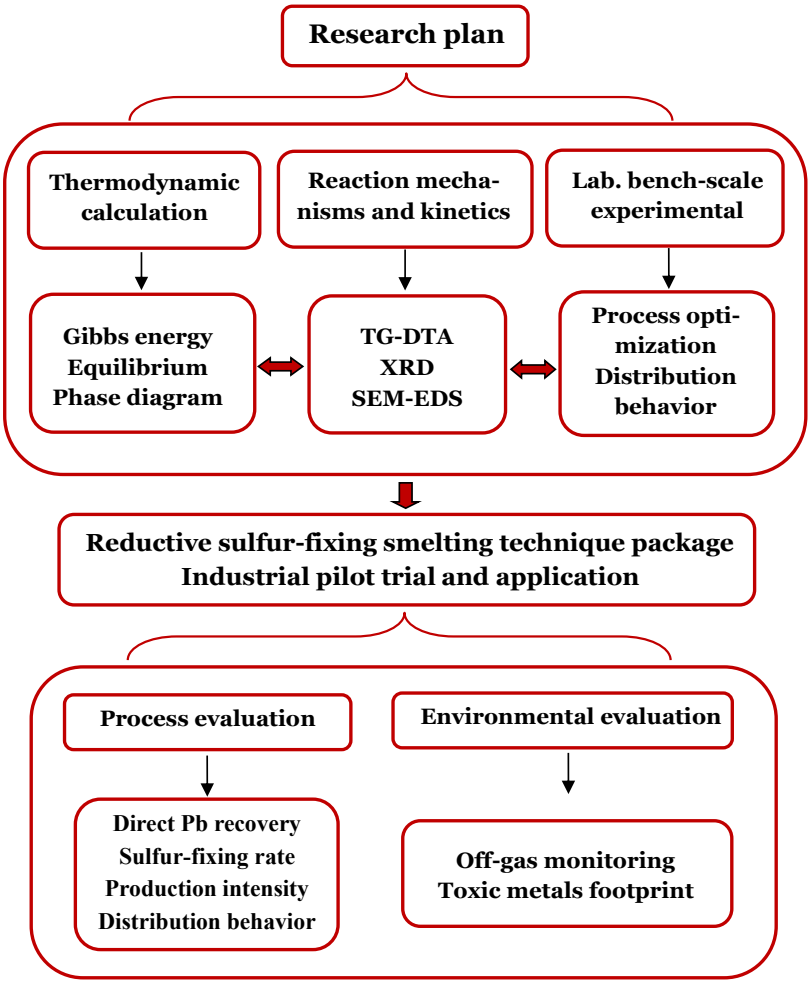


**Figure 2.** The study flowsheet in this thesis.

## 1.5 Practical application

The work conducted provides important knowledge regarding the reaction mechanisms of the studied systems and enables process optimization of LAB paste recycling. The above research technique and reaction mechanisms obtained can be applied for various scientific researches. This thesis provides extensive experimental data concerning the behaviors of lead and sulfur under various smelting conditions, which can be utilised to guide industrial practical applications.

This novel RSFS technique has been successfully implemented to recycle lead-containing secondary wastes and residues. It can also be extended to apply for smelting and extraction of antimony and bismuth from their primary concentrates, secondary materials, and recycling wastes, and at the same time, to co-treat different iron-, zinc-, copper-, nickel-containing (hazardous) wastes.

## 1.6 Structure of the thesis

This thesis consists of four scientific peer-reviewed journal papers (I-IV) included as appendices in this compendium at the end of this thesis. Chapter 1 briefly introduces the research background and reviews and discusses the previous investigations. The second chapter outlines the experimental procedure and setup, as well as the characterization method used for analysis of the samples. The obtained results of thermodynamic calculations, experimental kinetics, lab-scale bench experiments and industrial pilot trial and their discussions are presented in chapter 3. Chapter 4 summarizes the conclusions concerning the research conducted, followed by references.

# 2. Experimental

The core part of this chapter provides a detailed explanation of the experimental procedures and methods employed in this study. It includes the list of utilized chemicals and industrial raw materials and wastes, the stage primary-phase quenching method coupled with phase composition analysis (XRD and SEM-EDS) and arrangement of experimental setups used in reaction mechanism investigation. Publications (I-IV) by Yun Li et al. present detailed explanations of the methods for each particular system.

## 2.1 Materials

High purity chemicals were used to ensure a high experimental accuracy in the reaction kinetic mechanism study. All chemicals employed are listed in Table 1. Their mass fraction purities and suppliers are also presented. The pure chemicals in powder form were dried for 24 h to remove moisture and crystal water. The dry chemicals were then ground to -74 μm and prepared for analysis.

**Table 1.** Mass fraction purities and manufacturers of materials employed in the present study.

| Chemicals | Mass fraction purity/ wt% | Manufacturer |
|---|---|---|
| $PbSO_4$ | 99.99 | Alfa Aesar (Germany) |
| $Fe_2O_3$ | 99.95 | Aladdin Co., China |
| $Fe_3O_4$ | 99.96 | Aladdin Co., China |
| $Na_2CO_3$ | 99.99 | Alfa Aesar (Germany) |
| $Na_2SO_4$ | 99.0 | Aladdin Co., China |
| Carbon | 99.0 | Aladdin Co., China |
| CaO | 99.95 | Aladdin Co., China |
| $SiO_2$ | 99.99 | Alfa Aesar (Germany) |
| Alumina crucible | 99.98 | Taipingshengshi Co., China |
| Ar gas | 99.99 | Changsha Dingyi Co., China |
| $N_2$ gas | 99.99 | Changsha Dingyi Co., China |

Lead paste separated from spent LABs was employed as the major raw material in lab-scale batch processing tests. Two different iron-containing materials, i.e. hematite concentrate and JaR produced from zinc hydrometallurgy, were applied as sulfur-fixing agent. A metallurgical coke was employed as reductive agent. Simultaneously, various leaching residues (LR) produced from zinc hydrometallurgy were mixed with lead paste to synthesize a complex polymetallic material mixture. The mixture was used as feed material in the industrial pilot experiments to confirm the repeatability and reliability of this novel RSFS technique.

In addition, flux reagents, including $Fe_2O_3$, $Fe_3O_4$, CaO, and $SiO_2$, were used to adjust the slag system. Individual sodium salt $Na_2CO_3$ or a $Na_2CO_3$-$Na_2SO_4$ mixture was used to increase the fluidity of melt [70] and improve the smelting process. The chemical compositions and suppliers of the above materials are listed in Table 2. All amounts are given in weight percent (wt%). The XRD results of the materials are shown in detail in Publications I-IV.

**Table 2.** Chemical compositions and the suppliers of the corresponding materials.

| Materials | Chemical composition /wt% | | | | | | | | | Supplier |
|---|---|---|---|---|---|---|---|---|---|---|
| | Pb | S | Fe | Zn | Na | CaO | $SiO_2$ | Al | Ag* | |
| Lead paste A | 72.90 | 4.69 | 0.02 | 0.01 | 0.33 | 0.22 | 5.48 | 0.05 | -- | Yuguang Gold & Lead Co., China |
| Lead paste B | 68.81 | 3.33 | 0.05 | -- | 0.97 | 0.76 | 7.53 | 0.14 | -- | |
| Lead ash | 49.08 | 6.74 | 3.78 | 2.22 | -- | 0.39 | 0.89 | 0.17 | 45 | Guoda Nonferrous Metals Co., China |
| LR A | 30.51 | 12.19 | 3.77 | 6.72 | -- | 8.61 | 5.93 | 0.72 | 65 | |
| LR B | 18.56 | 0.72 | 8.89 | 0.42 | 1.14 | 0.79 | 44.13 | 4.78 | 35 | Guoda Nonferrous Metals Co., China |
| LR C | 11.61 | 2.17 | 12.41 | 0.36 | 0.34 | 7.83 | 6.84 | 0.81 | 730 | |
| Hematite | -- | 0.025 | 64.81 | 0.01 | 0.04 | 0.28 | 8.96 | 1.67 | -- | Xiangtan Iron & Steel Co., Ltd, China |
| JaR | 0.32 | 13.00 | 24.30 | 2.30 | 3.24 | 1.20 | 2.79 | 0.91 | 60 | Xingan Silver & Lead Co., China |
| Lead paste A | $PbSO_4$ | PbO | $PbO_2$ | Pb | | | | | | Yuguang Gold & Lead Co., China |
| | 54.68 | 8.49 | 22.05 | 8.53 | | | | | | |
| Lead paste B | 51.56 | 7.28 | 21.23 | 10.48 | | | | | | |
| Coke A | Fixed Carbon | | Volatile | | Ash | Fe | $SiO_2$ | $Al_2O_3$ | CaO | Xiangtan Iron & Steel Co., Ltd, China |
| | 84.05 | | 1.13 | | 13.94 | 15.96 | 30.96 | 18.18 | 4.05 | |
| Coke B | 81.27 | | 3.30 | | 15.43 | 25.23 | 41.23 | 6.60 | 25.24 | |

* Represented the unit is g/t;

The above analysis of the materials shows that the lead paste contained 68-73 % lead and 3.3-4.7 % sulfur. The main lead-bearing phases in the lead paste were $PbSO_4$ (51.6-54.7 %), $PbO_2$ (21.2-22.1 %), metallic Pb (8.5-10.5 %), and PbO (7.3-8.5%). In the lead-containing industrial wastes, the main lead-bearing phases were sulfate ($PbSO_4$), sulfide (PbS), oxide ($Pb_3O_4$ and $PbO_2$), and silicate ($PbSiO_3$). At the same time, zinc sulfate ($ZnSO_4$), zinc oxide sulfate ($Zn_3O(SO_4)_2$), iron sulfate ($Fe_2(SO_4)_3$), calcium sulfate ($CaSO_4$), a complex lead-zinc mineral queitite ($Pb_4Zn_2((SO_4)(SiO_4)(Si_2O_7))$), iron silicate ($FeSiO_3$), and ferric oxide ($Fe_2O_3$) were also detected. The hematite contained 88.0 % $Fe_2O_3$ (total iron 64.8 %) and its main impurity was $SiO_2$. JaR consisted of natrojarosite ($NaFe_3(SO_4)_2(OH)_6$), franklinite ($ZnFe_2O_4$), and zincbloedite ($Na_2Zn(SO_4)_2(H_2O)_4$.

## 2.2 Equipment

Reaction mechanism and laboratory batch-scale processing investigations were carried out in a horizontal tube furnace equipped with a gas and temperature controller (SR3-8P-N-90-100Z, SHIMADEN Co., Ltd., Japan, accuracy ±1 °C), as shown in Figure 3. Silicon carbide (SiC) heating elements were used to heat the furnace. Alumina crucible was used to carry the specimen. A S-type thermocouple in a re-crystallized alumina sheath was positioned immediately next to the specimen to measure the experimental temperature. The

left and right ends of the working tube were connected with gas flushing devices, and the flushing gas was inserted into the working tube from the right. The reaction mechanism investigation products were quenched in liquid $N_2$. The tail gas was absorbed by a NaOH solution.

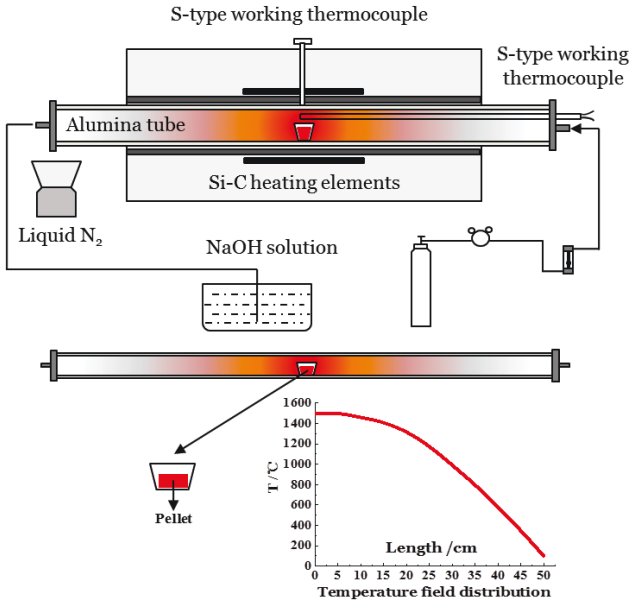


**Figure 3.** Schematic of the experimental apparatus and temperature profile of the furnace.

The industrial-scale experiments were conducted in a 4 $m^3$ blast furnace. A schematic of the process flow employed is shown in Figure 4.

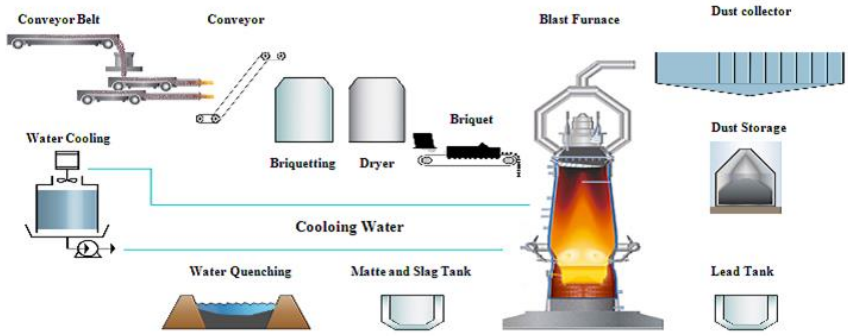


**Figure 4.** Schematic of the device connection in the industrial pilot trial campaign.

## 2.3 Methods

### 2.3.1 Experimental procedure

Pure $PbSO_4$ powder was selected as the raw material in the reaction kinetic mechanism studies, since it is the major as well as the most difficult compo-

nent to deal with in the spent lead paste. In order to reveal the reaction paths that may take place in each raw material component, sub-reaction systems with $PbSO_4$ involved were synthesized using pure chemicals according to their potential reaction stoichiometry. The synthetic mixtures were pressed uniaxially under 15 MPa into a cylindrical samples of 10 mm diameter.

In the laboratory batch -scale experiments, 200-300 g industrial lead paste or lead-containing secondary materials was mixed with a given amount of coke, hematite/JaR/PyC, sodium salt $Na_2CO_3$ or $Na_2CO_3$-$Na_2SO_4$ mixture, and other fluxes ($SiO_2$ and CaO). The mixture was placed in an alumina crucible. The crucible was pushed slowly into the constant temperature zone of the horizontal furnace at the desired temperature, after flushing with Ar, and held there for a preset time. The temperature was measured with a Pt–Rh thermocouple and controlled using a SHIMADEN SR25 Intelligent Temperature Controller (accuracy ± 1°C; Japan). The Ar gas flow during the reaction was fixed to 100 mL/min. After the preset reaction time, the product was taken out rapidly and quenched in liquid nitrogen. Different layers of the end product were carefully separated and weighed. The separated products were then crushed and prepared for analysis.

In the industrial pilot experiments, various lead-bearing secondary materials, including LAB paste, lead dust, lead sludge, and lead slag, were mixed carefully and briquetted with iron-containing wastes, e.g. PyC, JaR, goethite residue, various dusts produced from steel plant, and volatile kiln dust, etc., to obtain a mixture containing 30% Pb, 8% S, and 25% Fe. 1200 kg of dry briquettes were fed into the blast furnace with an appropriate amount of coke and fluxes (silica sand and limestone). The smelting products were discharged through their corresponding tap holes. Matte was laundered together with slag and settled in cast iron molds, see Figure 4. The slag floated on the surface of the matte, preventing oxidation. After tapping, the slag was quenched in a water pool.

### 2.3.2 Analytical methods

The dry pure $PbSO_4$ powder and the synthetic sub-reaction mixtures were subjected to TG-DTA analysis (STA 494 F3; NETZSCH, Germany) from 25°C to 1000°C at a heating rate of 10 °C /min and Ar flow rate of 100 mL/min.

Chemical compositions of the raw materials, lab-scale and industrial batch experimental products were analyzed using ICP-AES (Perkin Elmer, Optima 3000, Norwalk, USA). Prior dissolution of solid samples was carried out in nitrohydrochloric acid, a 3:1 mixture of concentrated HCl and $HNO_3$ aqueous solution, while shielding the influence of silica by hydrofluoric acid HF and perchloric acid $HClO_4$ treatment.

The phases of the products and also the reaction mechanism investigation samples were analysed by XRD (D/max 2550PC, Rigaku Ltd; Japan) with Cu-Ka radiation. The data were collected in the range of $2\theta$=10–80° with a $2\theta$ step width of 1°. The recorded patterns were evaluated using the PDF-2 powder diffraction pattern database [71].

The microstructures and chemical compositions of the representative products were identified by SEM-EDS analysis, (LEO 1450, Carl Zeiss, Germany,

INCA Wave 8570, Oxford Instruments, UK). The polished samples were carbon coated with a Leica EM SCD050 Coater (Leica Mikro system GmbH, Vienna, Austria) and analyzed immediately. The determination of different phases in the SEM images was based on EDS analysis results of 10 different points in the same mineral.

### 2.3.3 Calculation of the yields

In the batch experiments, the direct Pb recovery rate ($\eta$) and sulfur-fixing rate ($\gamma$) were calculated based on following equations (1) and (2), respectively:

$$\eta = \frac{\textit{Mass of Pb in the crude lead}}{\textit{Mass of Pb in the initial feed materials}} \times 100\% \quad (1)$$

$$\gamma = \frac{\textit{Mass of sulfur in the condensed solid smelting products}}{\textit{Mass of sulfur in the initial feed materials}} \times 100\% \quad (2)$$

# 3. Results and discussion

This chapter outlines the thermodynamic and kinetic information on extraction and recycling of lead from spent LAB paste and other polymetallic complex wastes for industrial practices and academic research. Thermodynamic and phase transformation mechanisms in the $PbSO_4$-$Fe_2O_3$-$Na_2CO_3$-C system and its subsystems are determined and clarified. A series of laboratory bench - scale experiments conducted, during the thesis work, to detect the influence of smelting conditions on lead extraction and sulfur fixation efficiency, are described. The obtained optimum smelting parameters obtained are discussed and their integration into the industrial pilot campaign is explained. Other potential industrial applications [72] of this novel RSFS technique are also summarized at the end of this chapter.

## 3.1 Thermodynamic calculation of RSFS process

### 3.1.1 Main reactions and Gibbs energy change

Among the raw materials employed in this investigation, the main lead-bearing phases in the feed materials are lead sulfate ($PbSO_4$), lead sulfide (PbS), and lead oxide (PbO and $PbO_2$). A series of reduction and sulfur-fixation reactions occur between the reactants in the smelting process [17]. The various reaction pathways are discussed and their reactions shown in Publication III. The Gibbs energy change $\Delta G_T^\theta$ of all above reactions was calculated using HSC Chemistry 9.2.6 and its database [73]. The results show that lead extraction and sulfur-fixation reactions in the presence of SFA, $Fe_2O_3$, and reductant are thermodynamically favorable. Increase in temperature is expected to promote the positive trends of the reactions. Metallic Pb can be extracted from $PbSO_4$, PbS, and PbO, and the sulfur in the initial raw materials can be transferred to FeS, $Na_2SO_4$, $Na_2S$ and $NaFeS_2$, and thus be fixed as ferrous matte, instead of emitting excessive amount of $SO_2$.

The reductive equilibrium diagrams of $PbSO_4$ and $Fe_2O_3$ at various reducing atmospheres based on the $\Delta G_T^\theta$ of the corresponding reactions are shown in Figure 5. A detailed description of the equilibrium diagram is presented in Publication I. Seven stability regions are observed to exist in different reducing atmospheres. $PbSO_4$ is easily reduced to PbS in reducing conditions. In the same domain, $Fe_2O_3$ is also reduced to $Fe_3O_4$. A large PbS + $Fe_3O_4$ co-existing region is found. As $P_{CO}/P_{CO_2}$ and temperatures are increased, Pb extraction

reactions take place between PbS and $Fe_3O_4$. Within this domain, metallic Pb, FeS, PbS, and $Fe_3O_4$ will coexist and sulfur will transfer from PbS to FeS.

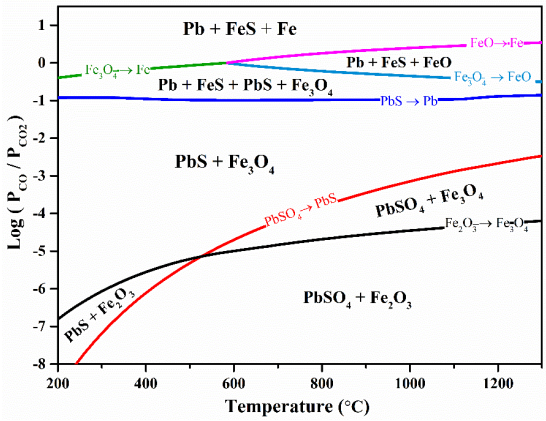


**Figure 5.** Reductive sulfur-fixing equilibrium diagram of $PbSO_4$ and $Fe_2O_3$.The data were obtained from HSC Chemistry 9.2.6 and its database.

### 3.1.2 Equilibrium compositions

The equilibrium compositions of the $PbSO_4$-$Fe_2O_3$-$Na_2CO_3$, $PbSO_4$-$Fe_2O_3$-C and the $PbSO_4$-$Fe_2O_3$-$Na_2CO_3$-C reaction systems are compared Figure 6.

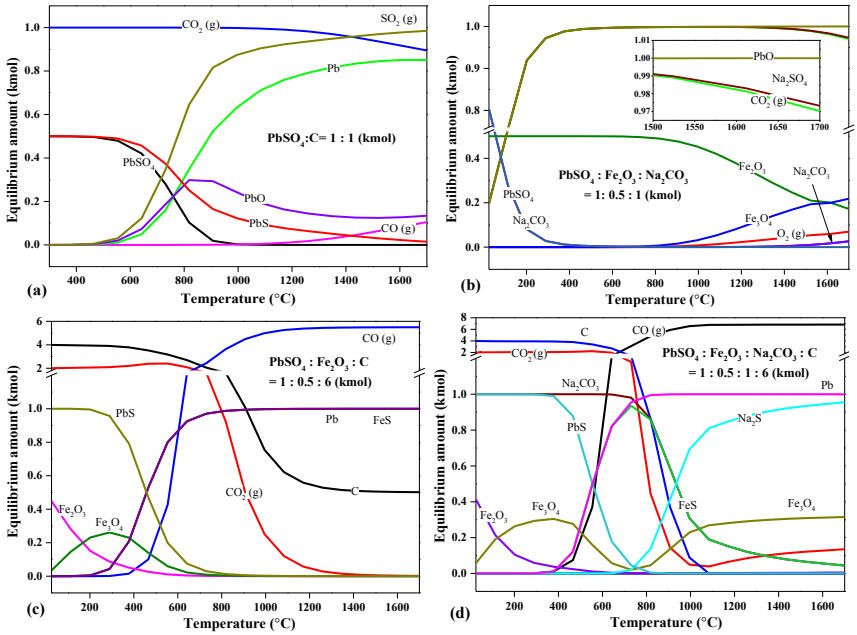


**Figure 6.** Equilibrium composition of (a) the $PbSO_4$ powder, (b) the $PbSO_4$-$Fe_2O_3$-$Na_2CO_3$ reaction system, (c) the $PbSO_4$-$Fe_2O_3$-C reaction system, and (d) the $PbSO_4$-$Fe_2O_3$-$Na_2CO_3$-C reaction system; the data was taken from HSC 9.2.6 and its database.

The equilibrium composition in Figure 6(a) indicates that without $Fe_2O_3$ and $Na_2CO_3$, a part of $PbSO_4$ is reduced to PbS and remaining $PbSO_4$ decomposes

to PbO and $SO_2$. As the temperature increases, lead extraction reaction occurs between PbS and PbO, metallic Pb is yielded. However, PbO is unable to be completely reduced to metallic Pb due to an insufficient carbon addition. Figure 6(b) suggests that in the absence of a reductant, $PbSO_4$ prefers to react with $Na_2CO_3$ to produce $Na_2SO_4$ and PbO even below 200 °C. Sulfur fixing agents, iron oxides, are not involved in any sulfur fixing reactions without carbon. Sulfur in $PbSO_4$ is transformed to $Na_2SO_4$ and is thus fixed in thus with the help of $Na_2CO_3$. No $SO_2$ is yielded. This implies that $Na_2CO_3$ can also fix sulfur and even function at low temperature.

Figure 6(c) indicates that without $Na_2CO_3$ addition, $PbSO_4$ and $Fe_2O_3$ are reduced to PbS and $Fe_3O_4$, respectively, before any reactions occur among them. Lead extraction and sulfur fixing reactions take place between PbS and $Fe_3O_4$. Finally, all lead and sulfur in initial $PbSO_4$ can be extracted and immobilized as metallic Pb and FeS, respectively. In case $Na_2CO_3$ and a reductant are both added together with $PbSO_4$, as shown in Figure 6(d), the sulfur fixing product FeS as well as the remaining PbS will further react with $Na_2CO_3$ after around 730 °C. Thus the amounts of Pb, $Na_2S$ and $Fe_3O_4$ products are seen to increase, while those of PbS, $Na_2CO_3$ and FeS decrease. This indicates that $Na_2CO_3$ is partly involved in the lead extraction reactions from PbS.

### 3.1.3 Phase diagrams

The phase diagrams of the $Fe_3O_4$-$Na_2O$-CaO-$Al_2O_3$-$SiO_2$ and Fe-$Fe_3O_4$-FeS systems are calculated by MTDATA ver. 6.0 [74] and MTOX database vers. 8.2 [75]. The phase diagram of the $Fe_3O_4$-$Na_2O$-CaO-$Al_2O_3$-$SiO_2$ system is presented in Figure 7 and the diagram of Fe-$Fe_3O_4$-FeS is shown in Publication II.

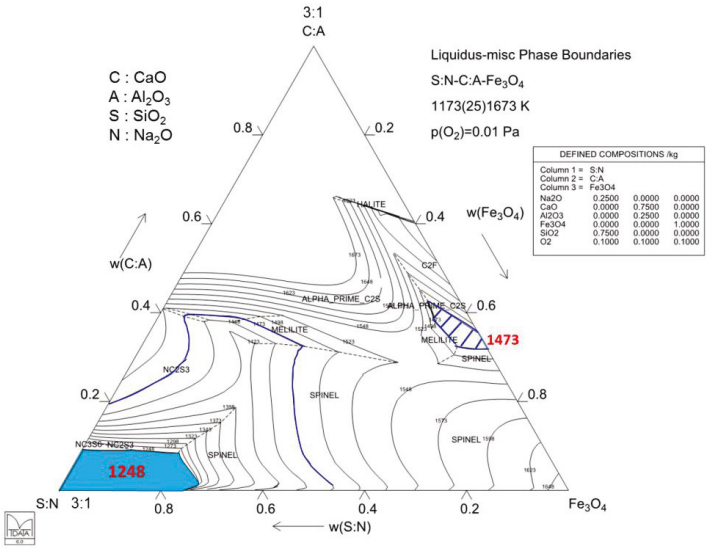


**Figure 7.** Phase diagram of the $Fe_3O_4$- $Na_2O$-CaO- $Al_2O_3$-$SiO_2$ system; the data was taken from MTDATA ver. 6.0 and its vers. 8.2 MTOX database.

Figure 7 indicates that the first liquid slag appears below around 975 °C (1248 K) surrounded by liquid $Na_2Ca_3(SiO_3)_6$, $Na_2Ca_2(SiO_3)_3$, and spinel ($Fe_3O_4$). It is a high-$SiO_2$ vitreous slag. This corresponds to the equilibrium state where PbS, FeS, metallic Pb, $Na_2SO_4$, and $Na_2S$, as shown in Figure 6, are generated in the smelting system. They stay in the liquid together with the remaining $Fe_3O_4$ and liquid $Na_2CO_3$. As the temperature increases further, more liquid is formed from $Na_2Ca_3(SiO_3)_6$, $Na_2Ca_2(SiO_3)_3$, spinel ($Fe_3O_4$) and other solid smelting materials. When the temperature reaches 1200 °C, melilite ($AlCaNaSi_2O_7$-$Al_2Ca_2SiO_7$-$Ca_2FeSi_2O_7$) also dissolve into the melt. Another liquid slag appears at 1200 °C surrounded by melitite, spinel $Fe_3O_4$, prime $Ca_2SiO_4$, and $Ca_2Fe_3O_6$. It is a low-$SiO_2$ slag and the liquid slag region expands with the temperature increases.

The phase diagram of Fe-$Fe_3O_4$-FeS presented in Publication II further reveals that the pyrrotite FeS melts may form in contact with spinel $Fe_3O_4$, wustite FeO (in the gragh: halite), or/and FCC-A1 Fe before 1000 °C (1273 K). A eutectic iron sulfide-oxide liquid appears and gradually expands along with temperature. At 1200 °C (1473 K), FeS is in liquid form. This promotes the generation of FeS and its settling from the smelting system as separate sulfide melt layer.

The above thermodynamic calculations reveal that lead extraction and simultaneous sulfur fixation from complex lead-containing materials is thermodynamically feasible. In the absence of a reducing agent, $Fe_2O_3$ does not participate in sulfur fixation. However, $Na_2CO_3$ is able to transfer $SO_3$ from $PbSO_4$ to $Na_2SO_4$ without carbon. Once the temperature increases and the atmosphere is sufficiently reducing, or in the absence of $Na_2CO_3$, $PbSO_4$ will be reduced to PbS. In this equilibrium state, PbS prefers to react with $Fe_3O_4$ instead of $Na_2CO_3$ to produce FeS and PbO. As the temperature exceeds 730 °C, the excess $Na_2CO_3$ will continue to react with FeS. The sulfur thus transfers from the initial $PbSO_4$ to PbS and then to FeS and $Na_2S$. As a result, the presence of $Na_2CO_3$ and reductant, as well as sulfur-fixing agent $Fe_3O_4$, can ensure efficient sulfur fixation and lead extraction at both low and high temperatures. The generation of $SO_2$ and $SO_3$ is significantly inhibited throughout the whole process. All lead can thus be extracted from $PbSO_4$ and PbS. A type of FeO-CaO-$Al_2O_3$-$SiO_2$-$Na_2O$ slag with low melting point and a $Fe_3O_4$ and PbS dissolved FeS-rich matte forms during smelting.

## 3.2 The phase conversion mechanisms and kinetics

The feasibility of lead extraction and sulfur fixation from lead paste, as calculated by thermodynamic softwares, was discussed in the previous section. In this section, the reaction path and rate of the reactions in the non-equilibrium states obtained experimentally are summarized.

### 3.2.1 $PbSO_4$-$Fe_2O_3$-C system

The phase transformation paths in the $PbSO_4$-$Fe_2O_3$-C system and its subsystems were identified by means of quenching method coupled with XRD and

SEM-EDS analysis. The thermogravimetric behaviors of above reaction systems were analyzed by TG-DTA. Full details of the experimental studies conducted during this work are in Publication I. Figure 8 presents a schematic of the reactions and phase conversion mechanisms in the $PbSO_4$-$Fe_2O_3$-C system based on the experimental analysis.

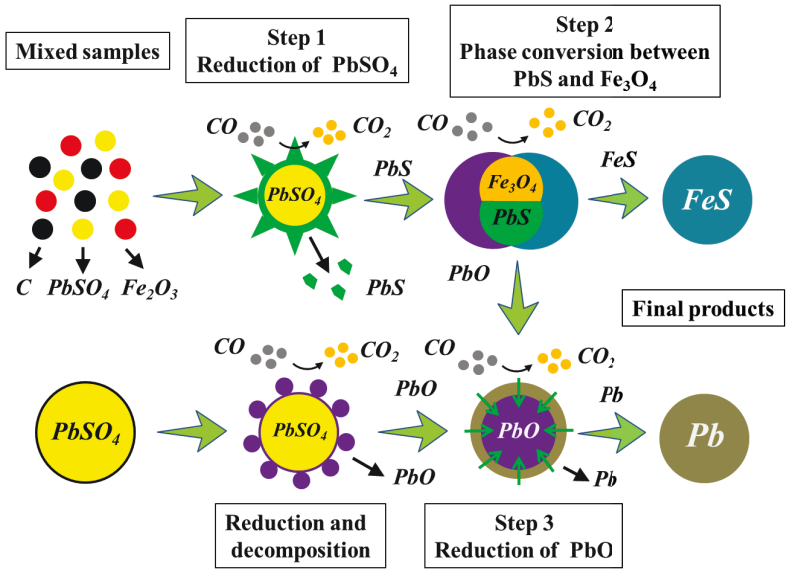


**Figure 8.** Reductive sulfur-fixing mechanism in the $PbSO_4$-$Fe_2O_3$-C reaction system.

$PbSO_4$ is first reduced to PbS, and $Fe_2O_3$ is reduced to $Fe_3O_4$ by carbon at high temperature. At the same time, some $PbSO_4$ also decompose to $PbO{\cdot}PbSO_4$ once the atmosphere is insufficiently reducing [76]. Next, the intermediate sulfide product, PbS, reacts with $Fe_3O_4$ to produce PbO and FeS. PbO is constantly reduced to metallic Pb. The reaction pathway cab be briftly described as $PbSO_4 \xrightarrow{C/CO} PbS \xrightarrow{Fe_3O_4} PbO \xrightarrow{C/CO}$ Pb. With the help of these exchange reactions, the sulfur in $PbSO_4$ is transferred to PbS, and is finally fixed and stabilized as FeS, which fundamentally prevents the generation of $SO_2$ gas. The experimental results agree well with the thermodynamic calculation results discussed in section 3.1. Some metallic Pb is also generated through the sequence $PbSO_4 \rightarrow PbO{\cdot}PbSO_4 \rightarrow 2PbO{\cdot}PbSO_4 \rightarrow 4PbO{\cdot}PbSO_4 \rightarrow PbO \rightarrow Pb$ by gas-solid processes.

The exchange reactions between PbS and $Fe_3O_4$ are the rate controlling step of the entire lead extraction process. A schematic of the exchange reactions between PbS and $Fe_3O_4$ is graphically shown in Figure 9. The presence of a reductant is essential and a sufficiently reductive atmosphere can selectively reduce $PbSO_4$ to PbS. It also facilitates the exchange reactions between PbS and $Fe_3O_4$ and ultimately generates metallic Pb and ferrous sulfide. These reactions guarantee sulfur conservation in the smelting system without formation of $SO_{2(g)}$ or $SO_{3(g)}$, and the subsequent discharge of sulfur into the atmosphere in the process off-gas.

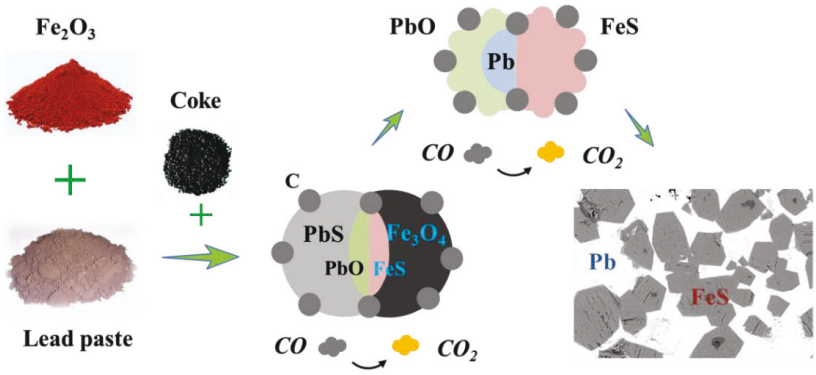


**Figure 9.** Phase transformation mechanism between PbS and $Fe_3O_4$.

### 3.2.2 $PbSO_4$-$Na_2CO_3$-C system

Equilibrium processes of the $PbSO_4$-$Na_2CO_3$-C system and its subsystems at different initial amounts are shown in Figure 10. Figure 10(a) reveals that the conversion reactions between $PbSO_4$ and $Na_2CO_3$ could occur without carbon at low temperature. $SO_3$ in $PbSO_4$ is transferred to $Na_2SO_4$ and is conserved in the system. In case the $Na_2CO_3$ addition is insufficient, unconverted $PbSO_4$ decomposes to PbO, $SO_2$ and $O_2$ at high temperature. When coke is present and with sufficient amount, as Figure 10(b) presents, $PbSO_4$ prefers to be reduced to PbS, instead of reacting with $Na_2CO_3$. Lead extraction reactions between PbS and $Na_2CO_3$ could also take place in the reducing atmosphere where the sulfur in PbS is transferred to $Na_2S$.

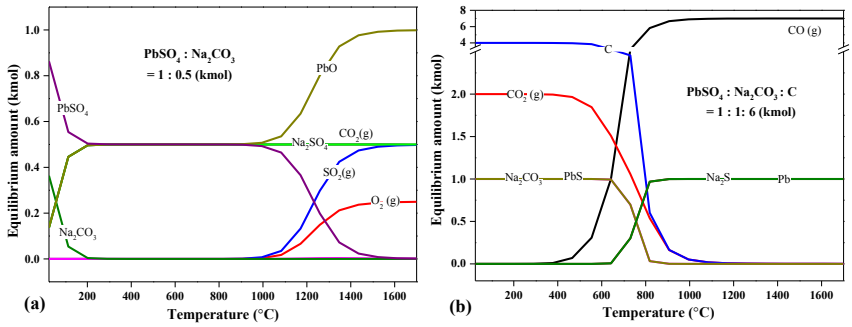


**Figure 10.** Equilibrium compositions of (a) $PbSO_4$-$Na_2CO_3$ mixture (molar ratio 1:0.5) and (b) $PbSO_4$-$Na_2CO_3$ -C mixture (molar ratio 1:1:6).

The detailed TG-DTA, XRD and SEM-EDS analysis results of $PbSO_4$-$Na_2CO_3$-C system and its subsystems are presented in Publication II. The reactions between $PbSO_4$ and $Na_2CO_3$ without carbon addition are a multistage process and follow the shrinking unreacted-core model, as show in Figure 11. The reacted $PbSO_4$ core is surrounded by liquid $Na_2CO_3$. The products $xPbO{\cdot}PbSO_4$ (x=1, 2 or 4) form a laminar boundary layer. PbO is generated from $PbSO_4$ through the following reaction sequence $PbSO_4 \rightarrow PbO{\cdot}PbSO_4 \rightarrow 2PbO{\cdot}PbSO_4 \rightarrow 4PbO{\cdot}PbSO_4 \rightarrow PbO$. Thus, $SO_3$ in $PbSO_4$ is transferred to

$Na_2SO_4$. The final products are stable PbO and $Na_2SO_4$ due to the absence of reductant. No metallic Pb is detected. These results agree well with the above thermodynamic equilibrium results.

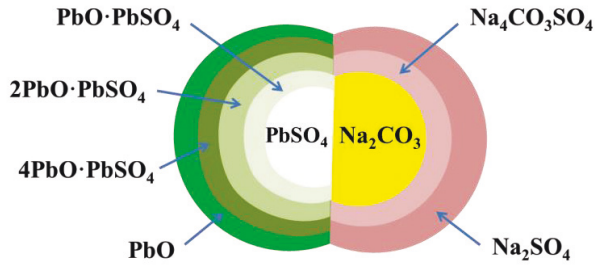


**Figure 11.** Multistage phase conversion mechanism in the $PbSO_4$-$Na_2CO_3$ mixture.

SEM-EDS results of the product in the $PbSO_4$-$Na_2CO_3$-C system at 750°C for 30 min reaction time are presented in Figure 12. It is observed that $(PbO)_x{\cdot}PbSO_4$ (x=1, 2 or 4) is close to $Na_2SO_4$ particles and a part of the $PbSO_4$ is reduced to PbS. Moreover, $(PbO)_x{\cdot}PbSO_4$ and $Na_2SO_4$ are surrounded by PbO and metallic Pb. This confirms that the reactions between $PbSO_4$ and $Na_2CO_3$ follow the shrinking unreacted-core model. $PbSO_4$ first reacts with $Na_2CO_3$ to generate $Na_2SO_4$ and PbO. $Na_2CO_3$ surrounds and gradually "erodes" $PbSO_4$ unreacted-core, and then the $PbSO_4$ core is disintegrated by molten $Na_2SO_4$. At the same time, the reaction product PbO gradually diffuses out from the unreacted $PbSO_4$ core.

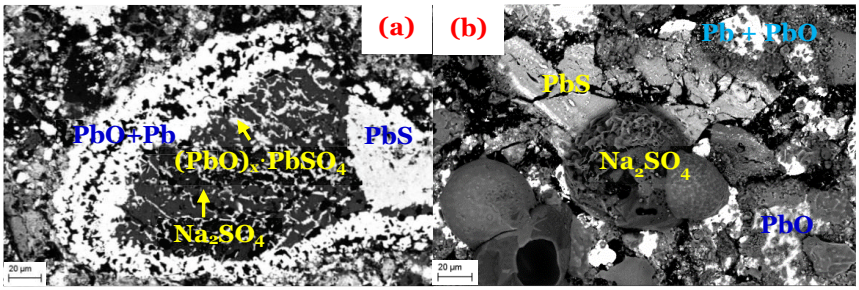


**Figure 12.** SEM micrographs of products in the $PbSO_4$-$Na_2CO_3$-C system at 750°C after 30 min reaction time.

### 3.2.3 $PbSO_4$-$Fe_2O_3$-$Na_2CO_3$-C system

The above reaction mechanisms in the $PbSO_4$-$Fe_2O_3$-C system and $PbSO_4$-$Na_2CO_3$-C system illustrate that lead extraction and sulfur fixing reactions can take place between PbS and $Fe_3O_4$ and also $PbSO_4$ and $Na_2CO_3$. In this section, the reaction mechanisms and experimental analysis of the entire $PbSO_4$-$Fe_2O_3$-$Na_2CO_3$-C system are discussed in detail.

Figure 13 illustrates the equilibrium composition of the $PbSO_4$-$Fe_2O_3$-$Na_2CO_3$-C system at different initial amounts. In a weakly reductive atmosphere, $PbSO_4$ is converted to PbO and $Na_2SO_4$ with the help of $Na_2CO_3$, while

PbS is also generated. However, the experimental XRD results of the $PbSO_4$-$Na_2CO_3$-C presented in Publication II reveal that it is difficult for carbon to function at low temperature because of the limited reaction kinetics; no PbS is detected until 750 °C after 30 min reaction. Therefore, in the non-equilibrium state, $PbSO_4$ will not be reduced to PbS at low temperature. Once temperature increases and the atmosphere is sufficiently reducing, PbO, PbS, Pb, $Na_2SO_4$, $Na_2CO_3$, $Fe_3O_4$ will co-exist in the system. A small amount of FeS, less than 0.1 kmol, is generated. This indicates that at low temperature or a weakly reductive atmosphere, the conversion reactions between $PbSO_4$ and $Na_2CO_3$ takes precedence over $PbSO_4$ reduction. Furthermore, the occurrence of exchange reactions between PbS and $Fe_3O_4$ is limited at weakly reductive atmospheres.

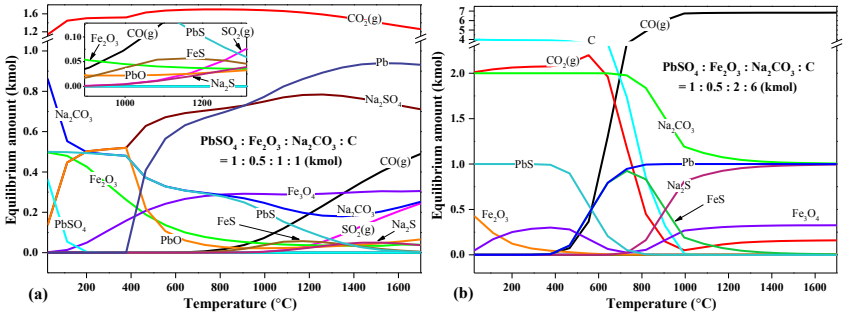


**Figure 13.** Equilibrium compositions of (a) $PbSO_4$-$Fe_2O_3$-$Na_2CO_3$-C mixture (molar ratio 1:0.5:1:1) and (b) $PbSO_4$-$Fe_2O_3$-$Na_2CO_3$-C mixture (molar ratio 1:0.5:2:6).

However, when the reductant addition is adequate and the temperature is high enough, as shown in Figure 13(b), $PbSO_4$ is reduced to PbS. At this condition, PbS, $Fe_3O_4$, and $Na_2CO_3$ co-exist. PbS prefers to react with $Fe_3O_4$ instead of $Na_2CO_3$ to generate metallic Pb and FeS. However, when temperature exceeds 630 °C, $Na_2CO_3$ gradually reacts with FeS as well as PbS. At the equilibrium conditions, all lead could thus be extracted from $PbSO_4$ and PbS below 800 °C once the carbon addition is sufficient.

The XRD patterns of the $PbSO_4$-$Fe_2O_3$-$Na_2CO_3$-C reaction system are presented in Figure 14. The results illustrate that the exchange reactions between $PbSO_4$ and $Na_2CO_3$ occur for the first time above 500 °C. At 650 °C $xPbO{\cdot}PbSO_4$ (x can be 1, 2 and 4), PbO and $Na_4CO_3SO_4$ are detected. These results are consistent with the previously discussed $PbSO_4$-$Na_2CO_3$-C system. With increased temperature, at 750 °C a part of $PbSO_4$ is reduced to PbS, and at the same time, PbO is reduced to metallic Pb. This indicates that the reductant has worked to reduce unconverted $PbSO_4$ and intermediate PbO. When temperature is increased to 850°C, $NaFeS_2$ is generated after 30 min reactions. This suggests that iron oxide is involved in the sulfur-fixation reactions. Sulfur in PbS and $Na_2SO_4$ is transferred to $NaFeS_2$. Metallic Pb emerges and is separated from the reaction mixture as a metal layer. When the temperature exceeds 1000 °C, intermediate products such as sodium iron oxides, sodium lead oxides and lead iron oxides are detected. The main products are Pb, $NaFeS_2$, FeS, $Na_2SO_4$ and PbS.

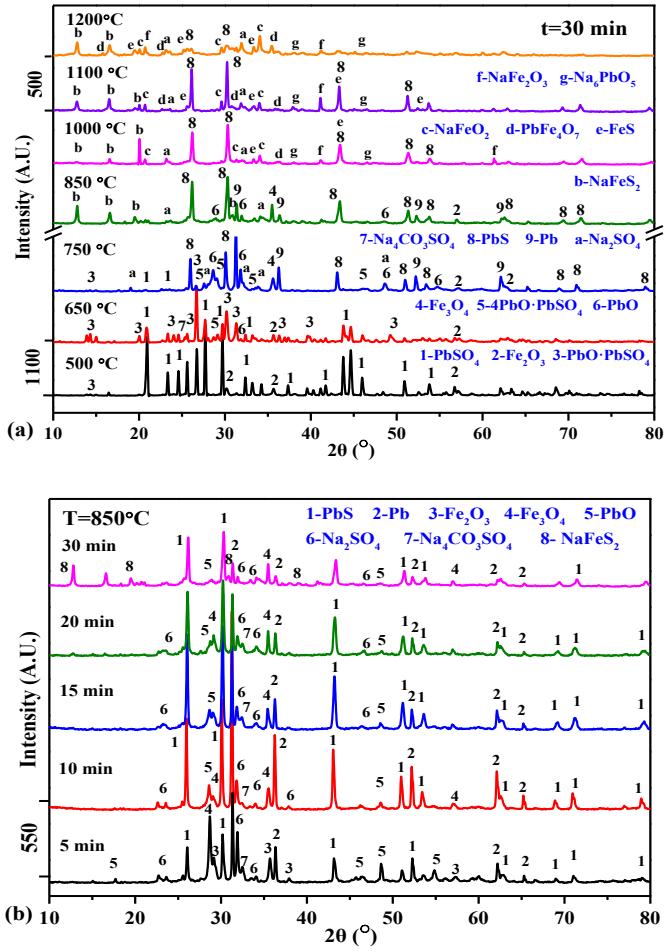


**Figure 14.** XRD patterns of products in $PbSO_4$-$Fe_2O_3$-$Na_2CO_3$-C (molar ratio 2:1:2:12) reaction system at (a) different temperatures and (b) with different reaction times.

Figure 14(b) suggests that $Na_2CO_3$ first reacts with $PbSO_4$ to convert it to PbO. At the same time, at 850°C, PbO is reduced to metallic Pb. The unconverted $PbSO_4$ is also reduced to PbS. After 5 min reaction, the products comprise of Pb, PbS, $Na_2SO_4$, PbO and $Fe_2O_3$. As reaction time extends, $Fe_3O_4$ emerged and metallic Pb steadily increase. However, $Fe_3O_4$ does not react with PbS for the first 20 min but only close to 30 min when $NaFeS_2$ emerges.

The phase transformation mechanism in $PbSO_4$-$Fe_2O_3$-$Na_2CO_3$-C reaction system is schematically presented in Figure 15. The presence of $Na_2CO_3$ and reductant is a critical factor to ensure sufficient sulfur fixation and lead recovery. At low temperatures and weakly reductive atmospheres, $PbSO_4$ first reacts with $Na_2CO_3$ to convert to PbO and $Na_2SO_4$, which avoids the decomposition of $PbSO_4$ and ensures the sulfur conservation in the system as sulfate without generating excessive fraction of sulfur as $SO_2$ gas. As temperature increases, unconverted $PbSO_4$ is selectively reduced to PbS [77-79]. Then, the sulfur-fixing agent, $Fe_3O_4$, reacts with PbS. The sulfur in PbS and $Na_2SO_4$ are further immobilized and finally recovered as FeS and $NaFeS_2$. The role of conversion

agent $Na_2CO_3$ at low temperature and sulfur fixing agent $Fe_2O_3$ at high temperature guarantee an efficient sulfur fixation yield in the smelting process.

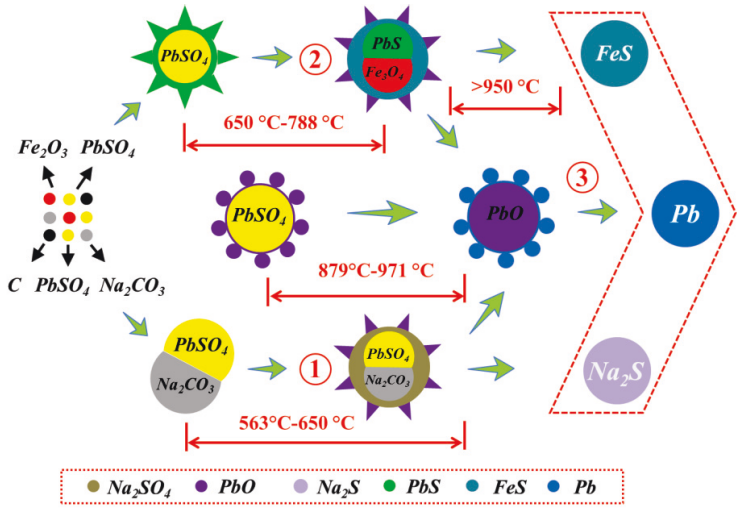


**Figure 15.** Phase transformations and microstructural evolution mechanism in the $PbSO_4$-$Fe_2O_3$-$Na_2CO_3$-C reaction system.

### 3.3 Lead paste recycling with sulfur fixation using hematite

Laboratory bench-scale experiments employing spent lead battery paste as raw material and hematite as SFA without $Na_2CO_3$ addition were conducted to investigate the influence of varying smelting conditions on lead extraction and sulfur-fixing efficiency. All material addition ratios are given in weight percent. The detailed experimental procedure is presented in Publication I. Figure 16 shows the direct lead recovery and sulfur fixing rate as a function of coke and hematite addition. An adequate coke and hematite addition is necessary to obtain an acceptable lead recovery and sulfur fixation. When coke addition is less than 10 % or hematite addition is less than 16 %, the formation of matte is limited and insufficient after 2 h smelting and settling times. The limited amount of matte obtained is difficult to separate from slag. At the same time, an insufficient reduction of lead oxides is detected in the matte and even the slag. Unreduced $Pb_2O_3$, PbO, and $Pb_2Fe_2O_5$ are entrained in the matte formed under 4% coke and 20% hematite addition at 1200 °C after 2 h smelting. An adequate reducing atmosphere is essential for lead recovery and sulfur fixation. The result is consistent with the thermodynamic and reaction mechanism results.

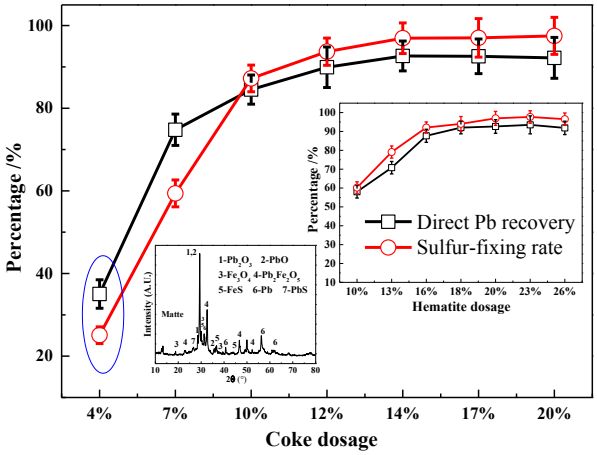


**Figure 16.** The effects of coke and hematite dosage on lead recovery and sulfur-fixing rates (1200°C, 2 h).

The laboratory bench-scale experiments with 2000 g lead paste were conducted without $Na_2CO_3$ addition under a condition of $W_{lead\ paste}$ : $W_{hematite}$ : $W_{coke}$ = 100 : 20 : 14 g, at a smelting temperature of 1200 °C and smelting time 3 h, to determine the repeatability of this novel process. Figure 17 presents a physical macrograph of the smelting products obtained. Three products, crude lead bullion, matte, and slag, are simultaneously obtained. Lead in the initial lead paste is extracted and enriched in lead bullion. Sulfur-fixing product forms the sulfide matte. The impurities in hematite and added the fluxes added form the slag. The products are visibly separated as three distinct layers. The compact slag floats on the surface of the condensed ferrous matte, and metallic Pb settles at the bottom due to density differences.

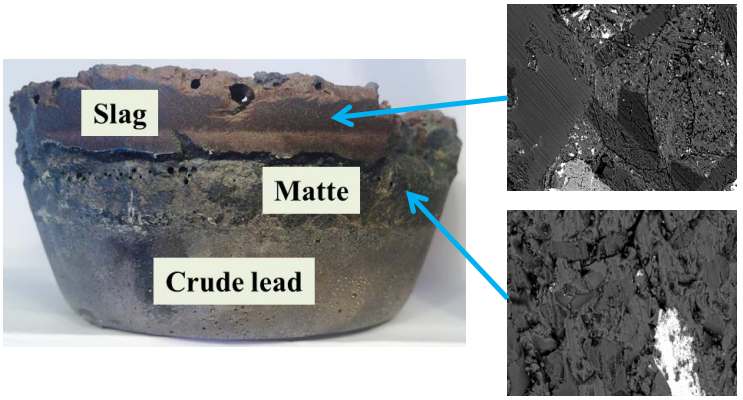


**Figure 17.** Physical macrograph of the smelting product obtained under condition of $W_{lead\ paste}$ : $W_{hematite}$ : $W_{coke}$ = 2000: 400 : 280 g, at 1200°C after 3 h.

The chemical compositions of the products obtained are shown in Table 3. The distribution behaviours of Pb, S, Fe, and Ba are presented in Figure 18. The results indicate that more than 93.1% lead in the raw materials is directly enriched in the crude lead bullion. 97.1% sulfur (90% in the matte and 7.1% in

the slag) is fixed as condensed sulfides. The purity of crude lead bullion reaches 98.9%, and lead concentrates in the matte and slag are below 4.1% and 1.2%, respectively. 77% iron is recovered in the matte, 21% stays in slag. 92.8% barium bearing from lead paste is distributed to slag. Therefore, hematite $Fe_2O_3$, not only plays a role of sulfur-fixing agent, but is also involved in slag-making.

**Table 3.** Chemical compositions of smelting products in the bench-scale experiments without $Na_2CO_3$ addition; other elements in the slag are Ca, Si, and Al ($W_{lead\ paste}$ : $W_{hematite}$ : $W_{coke}$ = 2000: 400 : 280 g, 1200°C, 3 h).

| No. | Product | Chemical compositions / wt% | | | | |
|---|---|---|---|---|---|---|
| | | Pb | Fe | S | Sb | Ba |
| 1 | | 99.03 | 0.033 | 0.07 | 0.072 | 0.001 |
| 2 | Crude lead | 98.89 | 0.078 | 0.09 | 0.098 | 0.001 |
| Average | | 98.96 | 0.056 | 0.08 | 0.085 | 0.001 |
| 1 | | 3.98 | 56.44 | 23.46 | -- | 0.05 |
| 2 | Ferrous matte | 4.06 | 56.89 | 24.66 | -- | 0.08 |
| Average | | 4.02 | 56.67 | 24.06 | -- | 0.07 |
| 1 | | 0.85 | 21.02 | 4.04 | -- | 0.98 |
| 2 | Slag | 1.17 | 23.12 | 3.90 | -- | 0.74 |
| Average | | 1.01 | 22.07 | 3.97 | -- | 0.86 |

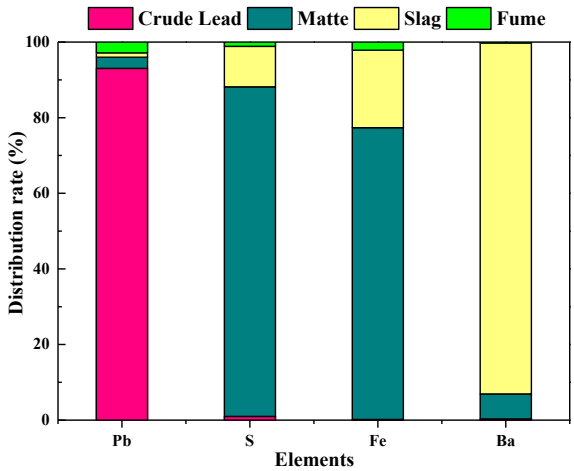


**Figure 18.** Distribution behaviors of Pb, S, Fe, and Ba in the bench experiment ($W_{lead\ paste}$ : $W_{hematite}$ : $W_{coke}$ = 2000: 400 : 280 g, 1200°C, 3 h).

Figure 19 shows the XRD patterns of the matte and slag obtained. It is observed that FeS is the major constituent of the matte; small diffraction peaks of Pb and $Fe_3O_4$ are also detected. The slag is comprised of $CaFeSiO_4$, $CaFe_4O_7$, $CaFe_2O_4$, $Fe_3O_4$, $Ca(Al_2Si_2O_8)$, $FeSiO_3$ and $Al_2O_3$. A little entrained PbS remains and is lost in the slag. Compared with the above mentioned matte generated in 4% coke addition in Figure 16, lead oxides are sufficiently reduced and recovered in an adequately reductive atmosphere. The production volume of matte is large enough to ensure a good settling and efficient lead recovery and sulfur fixation.

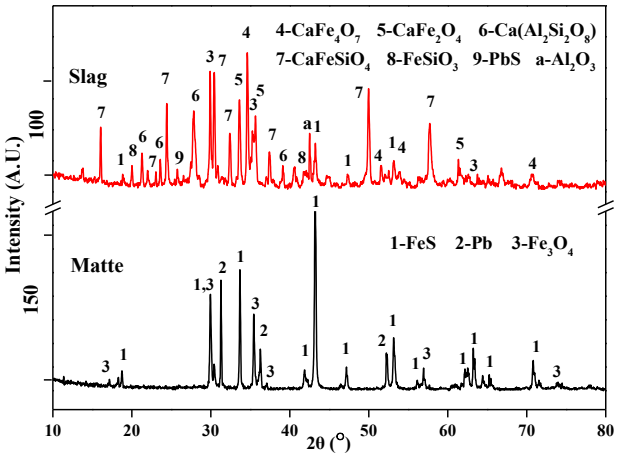


**Figure 19.** XRD patterns of the matte and slag obtained in the bench experiment ($W_{lead\ paste}$ : $W_{hematite}$ : $W_{coke}$ = 2000: 400 : 280 g, 1200°C, 3 h)

The SEM microstructure images of the recycling products obtained, the matte and slag, are presented in Figure 20. It is seen that the PbS is bonded to the FeS and is thus dissolved chemically in the matte. A small portion of FeS- and PbS-containing matte particles are also found entrained in $Ca(Al_2Si_2O_8)$ and $CaFe_4O_7$ of the slag. $Al_2O_3$ and CaO fuse with hematite $Fe_2O_3$, to form stable aluminium iron oxide ($Al_2Fe_2O_6$) and calcium iron oxides ($CaFe_2O_4$ and $CaFe_4O_7$), respectively. $FeSiO_3$ also bonds with CaO, and wollastonite $CaSiO_3$ combines with sillimanite $Al_2SiO_5$ to form kirschsteinite $CaFeSiO_4$ and anorthite $Ca(Al_2Si_2O_8)$, respectively. Barium tends to combine with $Al_2SiO_5$ in the slag.

The bench-scale experimental results validate the thermodynamic calculation and kinetic mechanism results. Metallic lead, sulfide matte and slag can be obtained at the same time in reducing atmosphere with sulfur conservation, instead of emitting excessive amount of $SO_2$. A reductive atmosphere is the critical parameter to guarantee an adequate formation volume of matte and exchange and reduction of lead paste.

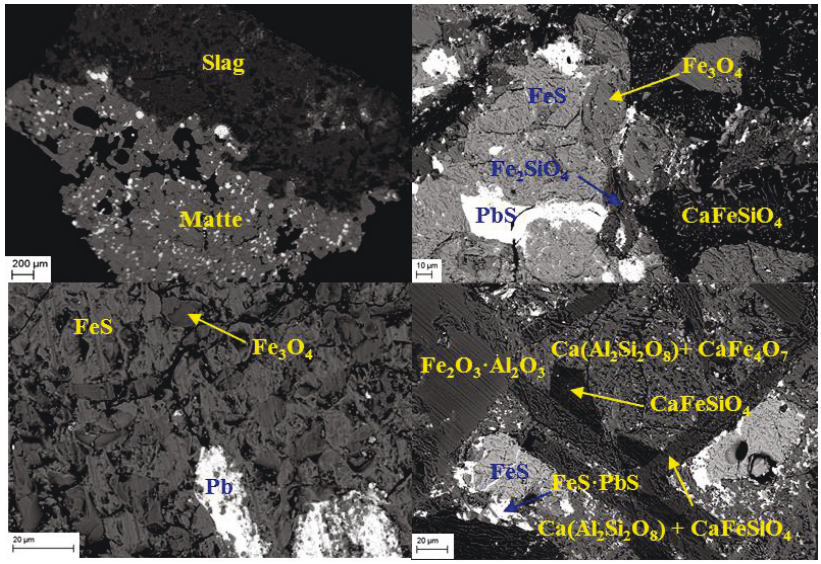


**Figure 20.** SEM results of the matte and slag produced in the bench-pilot experiments ($W_{lead\ paste}$ : $W_{hematite}$ : $W_{coke}$ = 2000: 400 : 280 g, 1200°C, 3 h)

## 3.4 Lead paste recycling and sulfur fixation with $Na_2CO_3$

Sodium salts, e.g. $Na_2CO_3$, NaCl, NaOH, are widely used as converters to pre-desulfurize lead paste in solution in hydrometallurgical recycling process [19]. $SO_3$ in $PbSO_4$ is transformed to $Na_2SO_4$ (aq) which can be crystallized out as a saleable by-product [4]. In the present study, sodium salt is used as a reaction mediate in the pyrometallurgical process to recycle LAB paste. The kinetic mechanism studies presented in Chapter 3.2 reveal that $Na_2CO_3$ is able to promote lead extraction and sulfur fixation efficiency [80]. The behavior and application of sodium salt in pyrometallurgy have been reported and discussed in [70, 81]. It has been shown to improve the fluidity and decrease viscosity and melting point of the melt [68, 82-85]. It also provides a flexible reaction medium and promotes the processing efficiency. In the present work, $Na_2CO_3$, coke, and sulfur-fixing agent were simultaneously added to the recycling system to convert and reduce lead paste as well as fix sulfur in a single process. This section summarizes the laboratory bench-scale experimental results obtained using hematite and further a jarosite residue as SFAs, respectively, with $Na_2CO_3$ addition.

### 3.4.1 Hematite

The effect of $Na_2CO_3$ addition on lead recovery and sulfur fixation from lead paste is shown in Figure 21. Direct lead recovery and sulfur-fixing rate increases from 79.9% and 90.7% to 94.2% and 96.9%, respectively, when 4% $Na_2CO_3$ is added. When the $Na_2CO_3$ addition exceeds 4%, lead recovery and sulfur-fixing rate remain constant at around 95% and 98%, respectively, after 1.5 h

smelting at 1200 °C. $Na_2CO_3$ addition improves lead extraction and simultaneously increases sulfur immobilization efficiency.

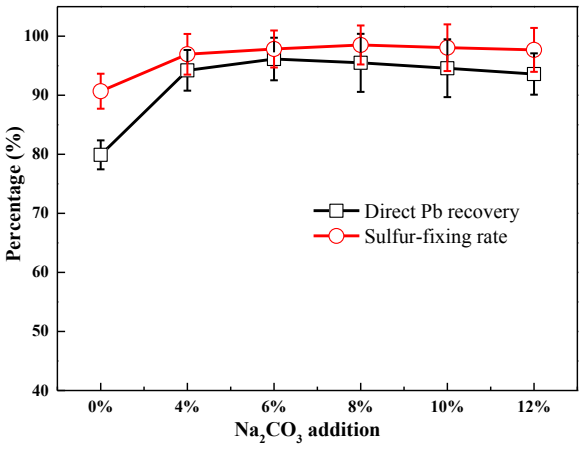


**Figure 21.** The effects of $Na_2CO_3$ dosage on lead recovery and sulfur-fixing rates ($W_{lead\ paste}$ : $W_{hematite}$ : $W_{coke}$ = 200: 40 : 24 g, 1200°C, 1.5 h)

The bench-pilot experiments with 1800 g lead paste were carried out to detect the repeatability and reliability of this process with $Na_2CO_3$ addition under a condition of $W_{lead\ paste}$ : $W_{hematite}$ : $W_{Na2CO3}$ : $W_{coke}$ = 100 : 20 : 4 : 12 g, at smelting temperature of 1200 °C and smelting time 1.5 h. The physical macrograph and the corresponding XRD patterns of smelting products are presented in Figure 22.

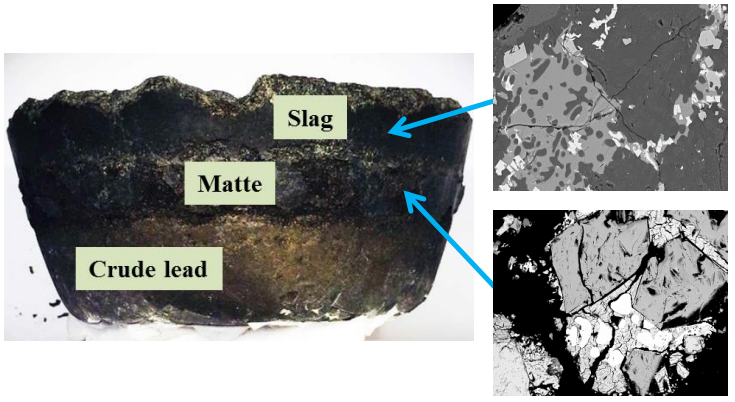


**Figure 22.** Physical macrograph of the recycling products obtained with $Na_2CO_3$ addition ($W_{lead\ paste}$ : $W_{hematite}$ : $W_{Na2CO3}$: $W_{coke}$ = 1800: 360 : 72 : 216 g, 1200°C, 1.5 h)

Compared with the products obtained without $Na_2CO_3$ addition, the matte obtained with $Na_2CO_3$ addition is a sulfide matte rich in $Na_2S$. The chemical compositions of different products obtained are shown in the Table 4. The detailed element distribution behaviors are presented in Publication II and summarized in Table 4.

**Table 4.** Chemical compositions of smelting products in the bench-scale experiments with $Na_2CO_3$ addition; other elements in the slag are Ca, Si, and Al ($W_{lead\ paste}$ : $W_{hematite}$ : $W_{Na2CO3}$: $W_{coke}$ = 1800: 360 : 72 : 216 g, 1200°C, 1.5 h)

| No. | Product | Chemical compositions / wt% | | | | | |
|---|---|---|---|---|---|---|---|
| | | Pb | Fe | S | Sb | Na | Ba |
| 1 | | 98.45 | 0.13 | 0.05 | 0.084 | -- | -- |
| 2 | Crude lead | 98.74 | 0.11 | 0.06 | 0.087 | -- | -- |
| Average | | 98.60 | 0.12 | 0.06 | 0.086 | -- | -- |
| 1 | | 2.69 | 52.53 | 22.72 | -- | 9.11 | 0.15 |
| 2 | Ferrous matte | 2.57 | 52.60 | 23.56 | -- | 9.40 | 0.18 |
| Average | | 2.63 | 52.57 | 23.14 | -- | 9.26 | 0.17 |
| 1 | | 0.46 | 23.67 | 2.51 | -- | 9.68 | 0.55 |
| 2 | Slag | 0.53 | 23.99 | 2.85 | -- | 9.78 | 0.57 |
| Average | | 0.50 | 23.83 | 2.68 | -- | 9.73 | 0.56 |

More than 96.2 % lead and 98.9 % sulfur (89.6 % in the matte and 9.3 % in the slag) in the raw materials are extracted and fixed within 1.5 h at 1200 °C. These are around 3% and 2% higher than the lead recovery and sulfur fixing rate, respectively, obtained without $Na_2CO_3$ addition. The generation and emission of excessive fraction of uts sulphur as $SO_2$ are significantly prevented. A crude lead bullion with a purity of 98% Pb is obtained. Lead contents in the matte and slag are decreased to 2.7 % and 0.6 %, respectively. These values are 1.4% and 0.6%, respectively, lower than the results obtained without $Na_2CO_3$. The kinetic mechanism study shows that the rate controlling step of lead extraction is the exchange reaction between PbS and $Fe_3O_4$, while $Na_2CO_3$ converts $PbSO_4$ to PbO. Therefore, a fraction of $PbSO_4$ will not be reduced to PbS in its absence. $Na_2CO_3$ helps break the controlling step and accelerate the lead recovery and also the sulfur fixation.

The XRD patterns and SEM-EDS analysis of the matte and slag are presented in Publication II. The major phase in the matte is FeS. The solidified slag is comprised of $Ca_2(Al(AlSi)O_7$, $Fe_2SiO_4$, $CaFe_4O_7$, $NaAlSiO_4$, $Na_2Si_2O_5$, $CaSiO_3$, $Fe_3O_4$, $Ca_2Al_2(SiO_4)_3$ and some entrained FeS. SEM-EDS results show that in the matte mackinawite FeS is bonded to magnetite $Fe_3O_4$. Sodium iron sulfide $NaFeS_2$ and galena PbS fill the gaps between magnetite. Metallic Pb is detected embedded in FeS and $NaFeS_2$. It is thus confirmed that lead extraction from PbS is carried out with the help of exchange reactions between $Fe_3O_4$ and PbS. In the slag, sodium aluminosilicate $NaAlSiO_4$ and sodium disilicate $Na_2Si_2O_5$ dissolved in fayalite $Fe_2SiO_4$ and gehlenite $Ca_2(Al(AlSi))O_7$. Mackinawite FeS is entrained in magnetite $Fe_3O_4$ and calcium iron oxide $CaFe_4O_7$ component, and magnetite is separated out from the fayalite matrix. The results agree well with the thermodynamic phase diagram calculation in Chapter 3.1.3 that FeS is in contact with $Fe_3O_4$ and melts together as an eutectic iron sulfide and oxide liquid. It separates out from $Fe_3O_4$ when temperature is decreased.

### 3.4.2 Jarosite residue

The experimental feasibility of using hematite concentrate as a SFA was validated in the previous sub-section. Hematite employed in this thesis was a high iron concentrate material with 64.8% Fe and 0.03% S. It has low levels of impurities. Therefore, the possibility of employing industrial iron-containing

wastes as SFA was also determined. Jarosite residue produced from zinc leaching procedure was selected as SFA to recover lead from lead paste with $Na_2CO_3$ addition. Chemical and phase compositing analysis results of JaR show that it contains 24.3% iron, 13% sulfur, and 2.3% zinc, and they are present as sulfate and oxide.

Figure 23 depicts the effect of coke and $Na_2CO_3$ dosage on lead recovery and sulfur-fixing rate using JaR as SFA. The results indicate that 91% lead and 92.6% sulfur are recovered and fixed under the condition of 8 wt% coke addition. When coke addition exceeda 8 wt%, lead recovery along with sulfur-fixing rate tenda to decline slightly, while the amount of lead lost in the slag decrease steadily. This indicates that the amount of lead in the matte and dust increases. Figure 24 presents the physical macrograph of the product obtained under a condition of $W_{lead\ paste} : W_{jarosite\ residue} : W_{Na2CO3} : W_{coke} = 200: 40 : 36 : 8$ g, at 1200°C after 2 h smelting time. A layer of $Na_2SO_4$ floats on the surface of slag. A small amount of matte bonds tightly with slag. 20% JrR addition is unable to provide sufficient iron to exchange lead from intermediate PbS and at the same time immobilize sulfur. On the contrary, excess sulfur is fixed as $Na_2SO_4$.

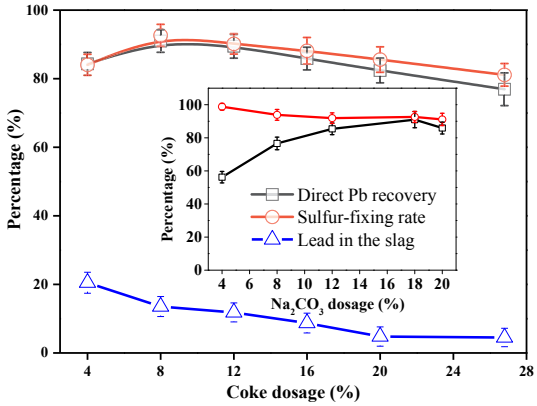


**Figure 23.** The effects of coke and $Na_2CO_3$ dosage on lead recovery and sulfur-fixing rates under a condition of $W_{lead\ paste} : W_{jarosite\ residue} : W_{Na2CO3} = 200: 40 : 36$ g, 1200°C, 2 h and $W_{lead\ paste} : W_{jarosite\ residue} : W_{coke} = 200: 40 : 16$ g, 1200°C, 2 h, respectively.


**Figure 24.** Physical macrograph of the products obtained under a condition of $W_{lead\ paste} : W_{jarosite\ residue} : W_{Na2CO3} : W_{coke} = 200: 40 : 36 : 8$ g, 1200°C, 2 h.

Additionally, when coke addition is fixed at 8%, lead recovery presents an upward trend as $Na_2CO_3$ dosage increases, whereas sulfur fixing rate remains constant at around 93%. Sufficient $Na_2CO_3$ addition can promote the conversion of $PbSO_4$ and enrichment of metallic lead. Compared with the results employing hematite as SFA, a little higher $Na_2CO_3$ dosage and lower coke addition is better for JaR to obtain a more efficient lead recovery and sulfur fixation due to the differences in their chemical and phase compositions.

Therefore, it is a promising option to treat JaR in the lead paste recycling process. Lead and sulfur are recovered, while some bearing valuable metals, e.g. Zn, Cu, Sb, Au, and Ag are also recycled.

### 3.5 Complex Pb-containing wastes recycling in $Na_2CO_3$-$Na_2SO_4$

The application of RSFS technique was further expanded to recycle more complex lead-containing wastes and residues, including lead ash, lead sludge, lead slag, and lead-silver-bearing iron sludge. Binary $Na_2CO_3$-$Na_2SO_4$ salt mixture was employed as reaction medium to improve the processing efficiency. The detailed experimental procedure and results are presented in Publication III [84].

The bench-pilot experiments with 200 g Pb-bearing mixture containing 30% Pb and 8% S were carried out under a condition of $W_{Pb\ (30\%)\ raw\ mixture}$ : $W_{coke}$ : $W_{Na2CO3+Na2SO4}$ = 200 : 30 : 18 g, $W_{Na2CO3}$ /$W_{Na2SO4}$=0.7/0.3, at smelting temperature 1200 °C and smelting time 2 h. An optical macrograph and XRD results of smelting products are illustrated in Figure 25.

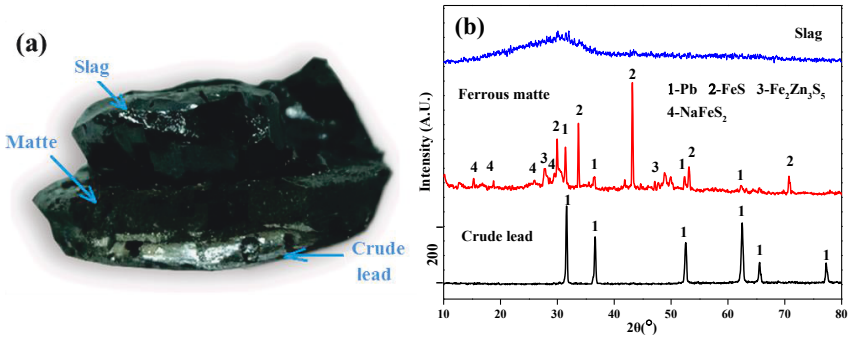


**Figure 25.** (a) Physical macrograph and (b) XRD patterns of the products in the bench-pilot experiments with $Na_2CO_3$-$Na_2SO_4$ addition ($W_{Pb\ (30\%)\ raw\ materials}$ : $W_{coke}$ : $W_{Na2CO3+Na2SO4}$ = 200 : 30 : 18 g, $W_{Na2CO3}$ /$W_{Na2SO4}$ = 0.7/0.3, smelting temperature 1200 °C, and smelting time 2 h)

The product is separated into three layers after cooling: vitreous slag, ferrous matte, and crude lead. The main components in the solidified matte are FeS, $NaFeS_2$, and $Fe_2Zn_3S_5$. Zinc is also involved in the sulfur-fixing relations and recycled as sulfide. The slag is a FeO-$SiO_2$-CaO-$Na_2O$ quaternary and is found to be solidified as a vitreous slag system. The chemical compositions of different products are presented in Table 5. Lead concentrate in the matte and slag are below 2.6% and 0.8%, respectively. Purity of the crude lead is higher than 96%, and its main impurity is metallic Fe. Compared with the lead bullion ob-

tained using hematite and JaR, the Pb purity decreases by around 1% because of a little higher coke addition in this investigation.

**Table 5.** Chemical compositions of smelting products in the bench-scale experiments with $Na_2CO_3$-$Na_2SO_4$ addition ($W_{Pb\ (30\%)\ raw\ mixture}$ : $W_{coke}$ : $W_{Na2CO3+Na2SO4}$ = 200 : 30 : 18 g, $W_{Na2CO3}$ /$W_{Na2SO4}$=0.7/0.3, smelting temperature 1200 °C, and smelting time 2 h)

| No. | Product | Chemical compositions / wt% | | | | | |
|---|---|---|---|---|---|---|---|
| | | Pb | Fe | S | Na | Zn | Ag* |
| 1 | Crude lead | 96.06 | 2.12 | 0.09 | 0.021 | 0.032 | 821 |
| 2 | | 97.02 | 1.72 | 0.12 | 0.024 | 0.039 | 845 |
| Average | | 96.54 | 1.92 | 0.11 | 0.023 | 0.036 | 833 |
| 1 | Ferrous matte | 2.54 | 48.80 | 24.07 | 7.47 | 2.36 | 89 |
| 2 | | 2.30 | 50.19 | 24.51 | 6.94 | 3.30 | 76 |
| Average | | 2.42 | 49.50 | 24.29 | 6.71 | 2.83 | 83 |
| 1 | Vitreous slag | 0.61 | 23.01 | 4.21 | 8.65 | 1.51 | <5 |
| 2 | | 0.72 | 24.58 | 3.07 | 8.24 | 1.83 | <5 |
| Average | | 0.67 | 23.80 | 3.64 | 8.45 | 1.67 | <5 |

* Represented the unit is g/t.

The distribution behaviors of Pb, Fe, Ag, S, Na and Zn in the bench-pilot experiments are presented in Figure 26. As shown, 92.4% Pb could be directly enriched in the crude lead, and only 5.5% and 1.8% of Pb is distributed into the ferrous matte and slag, respectively. 98.8% of Ag is also enriched in crude lead. 71.0% of iron is divided into ferrous matte as sulfide and the rest of 28.7% is in the FeO-$SiO_2$-CaO-$Na_2O$ slag. Total sulfur-fixing rate is 98.6% to condensed phases, with 91.3% in matte, 7.3% in slag. At the same time, 0.2% sulfur is in crude lead. Only 1.2% is distributed to the fume. Therefore, this novel RSFS process can significantly inhibit the generation of $SO_2$ and largely decrease the $SO_2$ emissions. Furthermore, 60.1% Na is distributed to slag, while 37.9% is conserved in matte as sulfide. Zinc scattered to matte, slag and dust with 31.9%, 42.8% and 24.8%, respectively.

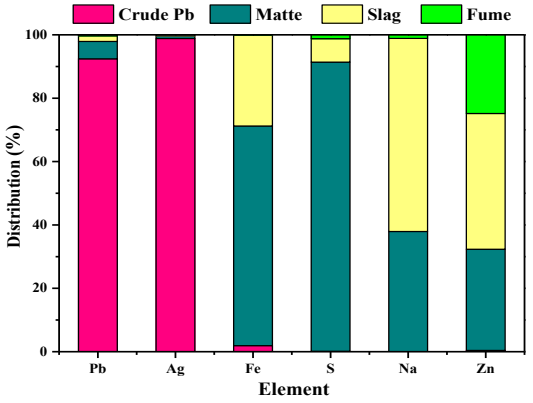


**Figure 26.** The distribution behaviors of Pb, Ag, Fe, S, Na and Zn in crude lead, ferrous matte, slag, and off-gas fume in the bench-pilot tests ($W_{coke}$ / $W_{Pb\ (30\%)\ raw\ materials}$ = 15%, $W_{Na_2CO_3 + Na_2SO_4}$ / $W_{Pb\ (30\%)\ raw\ materials}$= 18%, $W_{Na_2CO_3}$ / $W_{Na_2SO_4}$= 0.7/0.3, smelting temperature 1200 °C, and smelting time 2 h)

### 3.6 Industrial pilot trial and environmental evaluation

Laboratory bench-scale experimental studies confirm that the RSFS process is capable of producing lead bullion in high yield and purity from complex polymetallic lead-containing wastes with a wide range of initial material compositions (e.g. $PbSO_4$, PbS, PbO, $PbO_2$, and $PbSiO_3$) in an environmentally friendly manner. Gaseous $SO_2$ generation and emissions could thus be essentially controlled. The optimum smelting conditions obtained in laboratory bench-scale studies are summarized in Table 6.

**Table 6.** The optimum smelting conditions obtained from laboratory bench-scale studies on Lead-containing waste materials recycling process.

| Raw materials employed | Mixture ratio /g | Smelting temperature (°C) and time (h) | Reference |
|---|---|---|---|
| Lead paste : hematite : coke | 100: 20: 14 | 1200 °C, 3 h | Publication I |
| Lead paste : hematite : $Na_2CO_3$ : coke | 100 : 20 : 4 : 12 | 1200 °C, 1.5 h | Publication II |
| Lead sludge : lead ash : lead slag : iron sludge : (70% $Na_2CO_3$ + 30% $Na_2SO_4$) : coke | 48 : 23.9 : 5 : 23.1 : 18 : 15 | 1200 °C, 2 h | Publication III |
| Lead paste : pyrite cinder : $Na_2CO_3$ : coke | 100 : 25 : 4 : 12 | 1200 °C, 1.5 h | Publication IV |
| Lead paste : jarosite residue : $Na_2CO_3$ : coke | 100 : 25 : 18 : 8 | 1200 °C, 2 h | Reference 17 |

The above obtained optimum conditions, with different raw materials mixture, were integrated to carry out an industrial pilot trial to detect the reliability of RSFS technique and to evaluate its emissions' impact on the ecosystem [86]. The trial campaign was conducted in a 4 $m^3$ blast furnace with a scale of 1200 kg bench polymetallic materials mixture feed without sodium salt addition. The detailed experimental procedure is described in Chapter 2.3 and Publication I.

Figure 27 illustrates a time series of industrial tests to monitor the main chemical composition in the sulfide matte and slag. The results show that this process can be steadily executed on a continuous basis. Lead content in matte is approximately 4%-5%. Only 1-2% lead remains in the slag after one hour smelting time. At the same time, matte and slag enrichs 3%-5% and 3%-4% of zinc, respectively. Iron and sulfur content in matte can reach around 50% and 20%, respectively.

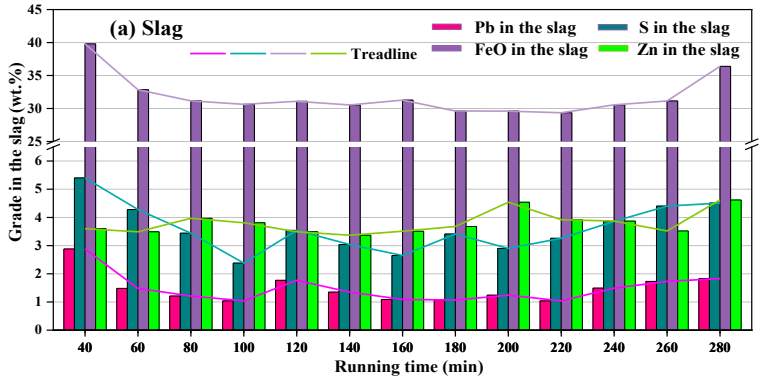

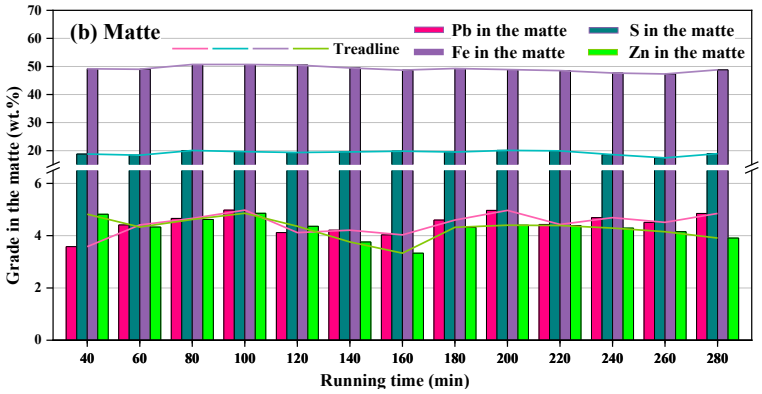


**Figure 27.** Chemical composition changes of the (a) slag and (b) matte produced during industrial pilot trial.

The key technical parameters of the industrial pilot campaign are listed in Table 7 and the distribution behaviors of the main components are presented in Figure 28, indicating that around 90% of the lead is directly recovered, i.e. the yields without subsequent slag cleaning and matte processing. A crude lead bullion with a purity of 96%-98% Pb is obtained in one step treatment. 97-99% of the sulfur in the feed is fixed in the condensed state, instead of generating and emitting excessive amount of $SO_2$ gas. This novel process offers advantages of low dust generation and high production capacity in currently available smelting furnaces.

**Table 7.** The key technical parameters of the industrial pilot campaign.

| Production intensity | Direct Pb recovery | Total Pb recovery | Dust rate | Sulfur-fixation rate | Coke consumption | Limestone consumption |
|---|---|---|---|---|---|---|
| kg/(m²·d) | % | % | % | % | kg/t Pb | kg/t Pb |
| 21000-33000 | 87-92 | 90-96 | 3-6 | 97-99 | 420-600 | 200-500 |

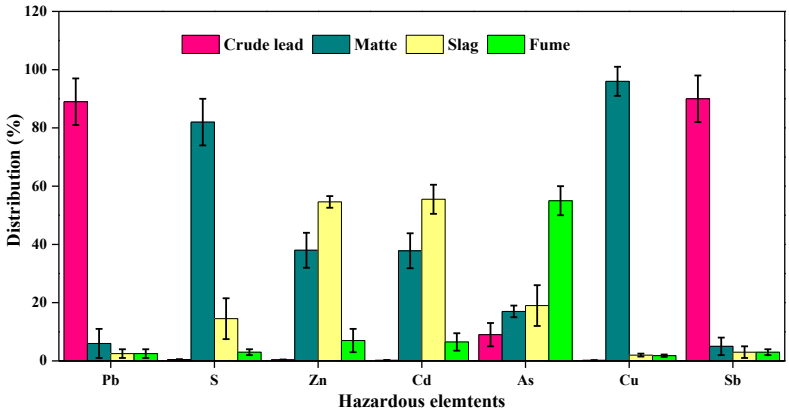


**Figure 28.** Distribution behaviors of the main components and hazardous elements during the industrial pilot campaign

The toxic elements fed from the lead-iron-containing wastes mainly contain Pb, Zn, Cu, Sb, As, Cd and S. As shown in Figure 28, around 54%-56% of Zn

distributes to slag, 35%-41% transfers to matte, 5%-9% of Zn volatilizes into fume; 47%-62% As volatilizes and is recovered in fume, 12%-22% transfers to slag, and only 18%-30% of As distributes to matte. The content of Cd in the raw materials is limited and its behavior is similar with Zn. Almost all Cu is enriched in matte. The behavior of Sb is similar with Pb, and mainly recovered in the crude lead. Therefore, the toxic metals of the feed and 97-99% of its sulfur transformed and distributed to crude lead, and to stable and marketable matte and slag. The ecological risk levels of the lead-iron-containing wastes decrease sharply in the reductive sulfur-fixing smelting treatment.

Table 8 shows the monitoring results of the blast furnace off-gas. It clearly reveals that hazardous Pb, Cd and $SO_2$ in the exhaust gas are lower than the emission standard GB 25466-2010 in China (National standard of P.R. China ---- Emission Standard of Pollutants for Lead and Zinc Industry).

**Table 8.** The blast furnace off-gas monitoring results during the pilot trial.

| Location of monitoring point | Monitored parameters | Monitoring results | | | | Executive standard |
|---|---|---|---|---|---|---|
| Blast furnace smoke window | Pb / (mg/m³) | 0.046 | 0.041 | 0.034 | 0.037 | 0.5 |
| | $SO_2$ / (mg/m³) | 380 | 363 | 354 | 372 | 400 |
| | Cd / (mg/m³) | 0.00019 | 0.00017 | 0.00021 | 0.00016 | 0.05 |
| | Blackness | <1 | <1 | <1 | <1 | <1 |

The smelting products in the industrial pilot campaign contain crude lead bullion, matte, water-quenched slag, and dust. The main product, lead bullion will be subjected to electrorefining process to product high purity lead (≥99.99%). The dust returns to the smelting process as raw material. The slag is sold to cement making as a raw material for clinker production after water-quenching and granulation. The matte produced can be sold directly to cast ballast, or subjected to sulfuric acid plant to recover sulfur and combustion energy, and at the same time regenerate sulfur-fixing agent. No harmful wastes are stockpiled and as reverts in the plant. The only emission is the standard-conformed $SO_2$-containing off gas. The environmental risk is thus very low. The reductive sulfur-fixing smelting process is therefore a potentially effective technology for both recovering metals and protecting the environment in LAB recycling.

Recently, this novel Pb recycling process was industrially adopted [72] in several recycling plants in China, such as Guoda Nonferrous Metals Metallurgy Co., Ltd. China and Yongchang Precious Metals Co., Ltd. China [87]. It has proved feasible in industrial use. The off-gas emissions met the relevant Chinese standards. Moreover, in addition to lead-containing wastes recycling, this novel technique can also be used for treating antimony- [28,30], bismuth- [40], zinc- [41], and copper-containing [42] wastes and residues. It is therefore a promising alternative recycling and treatment method for various waste (hazardous) materials and residues.

# 4. Conclusions

A novel and cleaner lead-acid battery paste recycling technique by reductive sulfur-fixing recycling was proposed. Thermodynamic calculations, including Gibbs energy change, equilibrium composition, and phase diagram, were conducted to build the thermodynamic fundamentals. Experimental determination of the reaction mechanisms and kinetics in the $PbSO_4$-$Fe_2O_3$-C, $PbSO_4$-$Na_2CO_3$-C, and $PbSO_4$-$Fe_2O_3$-$Na_2CO_3$-C systems were carried out with the help of thermogravimetric analysis and quenching method coupled with XRD and SEM-EDS analysis.

The reaction mechanism and obtained kinetic results showed that the lead extraction and sulfur fixing reactions followed the shrinking unreacted-core model. The presence of $Na_2CO_3$ helped to transform $SO_3$ from $PbSO_4$ to $Na_2SO_4$ at low temperatures and in weakly reductive atmospheres. This ensured the conservation of sulfur in the smelting system without emitting excessive fraction of its sulfur as $SO_2$ to the atmosphere. Once the atmosphere was sufficiently reductive or without $Na_2CO_3$ addition, $PbSO_4$ was reduced to PbS. Next, the sulfur-fixing agent $Fe_3O_4$ reduced from $Fe_2O_3$ reacted with PbS to exchange sulfur to FeS, and at the same time, PbS converted to PbO. Finally, metallic lead was extracted from PbO, and $Na_2SO_4$ was reduced to $Na_2S$. Part of FeS bonded with $Na_2S$ to form $NaFeS_2$. Consequently, sulfur was fixed as FeS, $NaFeS_2$, $Na_2S$ or $Na_2SO_4$, instead of generating $SO_2$.

Laboratory bench-scale experiments were conducted to find out the influences of each smelting condition on lead extraction and sulfur fixation efficiency. The optimum process parameters for LAB paste recycling were obtained. Furthermore, the application of this new technique was extended to recycle and co-treat various complex lead-iron-zinc-containing waste materials and residues. The results indicate that cleaner and effective extraction of lead from complex polymetallic wastes using reductive sulfur-fixing smelting process was fundamentally and experimentally feasible.

Three clearly stratified smelting products, crude lead, ferrous matte, and slag, were obtained simultaneously in this novel process. While 91%-96% lead was recovered in crude lead bullion, and 97%-99% sulfur was fixed in the condensed matte and slag as sulfide. Purity of the crude lead reached 96%-98%, and its main impurity was metallic Fe. At the same time, lead concentration in the ferrous matte and slag were below 2.4%-4.1% and 0.5-1.2%, respectively. The addition of sodium salts, e.g. $Na_2CO_3$ and $Na_2CO_3$-$Na_2SO_4$ mixture, pro-

moted the reductive sulfur-fixing process. Lead extraction and sulfur-fixation efficiency were improved.

The industrial pilot campaign was also carried out. The results showed that this process can be steadily executed on a continuous basis and offered advantages of low dust generation and high production capacity in currently available smelting furnaces. The operating expenditure was reduced significantly. The off-gas emissions met the relevant Chinese standards. It was possible to recover 90-96% of lead in one step treatment to crude lead, without subsequent slag cleaning and matte processing. The lead content of matte and slag was around 4-5% and 1-2%, respectively. The sulfur-fixation rate reached 97-99%, and excessive gaseous $SO_2$ emissions could be essentially eliminated. Furthermore, the toxic metals in the feed transform and distribute to crude lead, and stable and marketable matte and slag. The ecological risk levels of the lead-iron-containing wastes decreases sharply after the reductive sulfur-fixing smelting treatment.

The reductive sulfur-fixing smelting process is a potentially effective technology for both recovering metals and protecting the environment. In addition to LAB paste recycling, this new process provides a promising alternative recycling and treatment for various waste (hazardous) materials and residues containing lead, iron, zinc, antimony, bismuth, and copper. It is an environment-friendly and high-efficiency technique that offers multiple application in the fields of materials recycling.

# References


[1] G.J. May, A. Davidson, B. Monahov, Lead batteries for utility energy storage: A review, J. Energy Storage, 15 (2018) 145-157.

[2] R. Peng, H.J. Ren, X.P. Zhangs, Metallurgy of lead and zinc, Beijing: Sci. Pres., China, 2003.

[3] X. Tian, Y. Wu, Y. Gong, T. Zuo, The lead-acid battery industry in China: outlook for production and recycling, Waste Manage. & Res., 33 (2015) 986-994.

[4] W. Zhang, J. Yang, X. Wu, Y. Hu, W. Yu, J. Wang, J. Dong, M. Li, S. Liang, J. Hu, A critical review on secondary lead recycling technology and its prospect, Renew. Sustain. Energ. Rev., 61 (2016) 108-122.

[5] A.D. Ballantyne, J.P. Hallett, D.J. Riley, N. Shah, D.J. Payne, Lead acid battery recycling for the twenty-first century, Roy. Soc. Open Sci., 5 (2018) 171368.

[6] S. Ji, C. Cherry, M. Bechle, Y. Wu, J.D. Marshall, Electric vehicles in China: emissions and health impacts, Environ. Sci. Technol., 46 (2012)2018-2024.

[7] Z. Sun, H. Cao, X. Zhang, X. Lin, W. Zheng, G. Cao, Y. Sun, Y. Zhang, Spent lead-acid battery recycling in China - A review and sustainable analyses on mass flow of lead, Waste Manag., 64 (2017) 190-201.

[8] F. Chen, B. Yang, W. Zhang, J. Ma, J. Lv, Y. Yang, Enhanced recycling network for spent e-bicycle batteries: A case study in Xuzhou, China, Waste Manag., 60 (2017) 660-665.

[9] X. Tian, Y. Wu, Y. Gong, T. Zuo, The lead-acid battery industry in China: outlook for production and recycling, Waste Manag. Res., 33 (2015) 986-994.

[10] Q. Zhang, The current status on the recycling of lead-acid batteries in China, Int. J. Electrochem Sci., 8 (2013) 6457-6466.

[11] X. Zhu, X. He, J. Yang, L. Gao, J. Liu, D. Yang, X. Sun, W. Zhang, Q. Wang, R.V. Kumar, Leaching of spent lead acid battery paste components by sodium citrate and acetic acid, J. Hazard. Mater., 250 (2013) 387-396.

[12] D.C.R. Espinosa, A.M. Bernardes, J.A.S. Tenório, An overview on the current processes for the recycling of batteries, J. Power Sources, 135 (2004) 311-319.

[13] K.P. Jeong, J.G. Kim, Lead acid battery recycling and material flow analysis of lead in Korea, J. Mater. Cy. Waste Manag., 16(2017) 1-7.

[14] T.W. Ellis, A.H. Mirza, The refining of secondary lead for use in advanced lead-acid batteries, J. Power Sources, 195 (2010) 4525-4529.
[15] R.A. Huggins, Lead-Acid Batteries, Springer US, 2016.
[16] Y. Li, Y. Chen, C. Tang, S. Yang, L. Klemettinen, M. Rämä, X. Wan, A. Jokilaakso, A New Pyrometallurgical Recycling Technique for Lead Battery Paste Without $SO_2$ Generation—A Thermodynamic and Experimental Investigation, in: Extraction 2018, Springer, 2018, pp. 1109-1120.
[17] Y. Li, C. Tang, Y. Chen, S. Yang, L. Guo, J. He, M. Tang, One-Step Extraction of Lead from Spent Lead-Acid Battery Paste via Reductive Sulfur-Fixing Smelting: Thermodynamic Analysis, in: 8th International Symposium on High-Temperature Metallurgical Processing, Springer, 2017, pp. 767-777.
[18] D. Lin, K. Qiu, Recycling of waste lead storage battery by vacuum methods, Waste Manag., 31 (2011) 1547-1552.
[19] W. Yu, P. Zhang, J. Yang, M. Li, Y. Hu, S. Liang, J. Wang, S. Li, K. Xiao, H. Hou, A low-emission strategy to recover lead compound products directly from spent lead-acid battery paste: Key issue of impurities removal, J. Clean. Prod., 210 (2019) 1534-1544.
[20] P. Frohlich, T. Lorenz, G. Martin, B. Brett, M. Bertau, Valuable Metals-Recovery Processes, Current Trends, and Recycling Strategies, Angew. Chem. Int. Ed. Engl., 56 (2017) 2544-2580.
[21] M. Li, J. Liu, W. Han, Recycling and management of waste lead-acid batteries: A mini-review, Waste Manag. Res., 34 (2016) 298-306.
[22] B. Blanpain, S. Arnout, M. Chintinne, D. R. Swinbourne, Lead Recycling, In: Handbook of Recycling, Elsevier, Boston, 2014, pp.95-111.
[23] C.S. Brooks, Metal recovery from industrial waste, CRC. Press., 2018.
[24] L. Zhang, Z. Xu, A review of current progress of recycling technologies for metals from waste electrical and electronic equipment, J. Clean. Prod., 127 (2016) 19-36.
[25] Z. Sun, Y. Xiao, H. Agterhuis, J. Sietsma, Y. Yang, Recycling of metals from urban mines–a strategic evaluation, J. Clean. Prod., 112 (2016) 2977-2987.
[26] M. Ciftci, B. Cicek, E-waste: A Review of CRT (Cathode Ray Tube) Recycling, Research & Reviews: J. Mater. Sci., 05 (2017)1-17.
[27] T.J. Van der Kuijp, L. H., C.R. Cherry, Health hazardous of China's lead-acid battery industry: a review of its market drivers, production processes, and health impacts, Environ. Health, 12 (2013) 61-71.
[28] X. Tian, Y. Wu, P. Hou, S. Liang, S. Qu, M. Xu, T. Zuo, Environmental impact and economic assessment of secondary lead production: Comparison of main spent lead-acid battery recycling processes in China, J. Clean. Prod., 144 (2017) 142-148.
[29] Z. Sun, H. Cao, X. Zhang, X. Lin, W. Zheng, G. Cao, Y. Sun, Y. Zhang, Spent lead-acid battery recycling in China–A review and sustainable analyses on mass flow of lead, Waste Manag., 64 (2017) 190-201.

[30] A.L. Wani, A. Ara, J.A. Usmani, Lead toxicity: a review, Interdiscip. Toxicol., 8 (2015) 55-64.
[31] T. Liu, K. Qiu, Removing antimony from waste lead storage batteries alloy by vacuum displacement reaction technology, J. Hazard. Mater., 347 (2018) 334-340.
[32] M.L. Jaeck, Primary and Secondary Lead Processing: Proceedings of the International Symposium on Primary and Secondary Lead Processing, Halifax, Nova Scotia, Elsevier, 2013.
[33] J. Wei, X. Guo, D. Marinova, J. Fan, Industrial $SO_2$ pollution and agricultural losses in China: evidence from heavy air polluters, J. Clean. Prod., 64 (2014) 404-413.
[34] Y. Zhang, S. Li, Z. Chen, F. Wang, J. Chen, L. Wang, A systemic ecological risk assessment based on spatial distribution and source apportionment in the abandoned lead acid battery plant zone, China, J. Hazard. Mater., 354 (2018) 170-179.
[35] H. Zakiyya, Y. Distya, R. Ellen, A review of spent lead-acid battery recycling technology in Indonesia: Comparison and recommendation of environment-friendly process, in: IOP Conference Series: Materials Science and Engineering, IOP Publishing, 2018, pp. 012074.
[36] R. Prengaman, A. Mirza, Recycling concepts for lead–acid batteries, in: Lead-Acid Batteries for Future Automobiles, Elsevier, 2017, pp. 575-598.
[37] X. Zhang, L. Li, E. Fan, Q. Xue, Y. Bian, F. Wu, R. Chen, Toward sustainable and systematic recycling of spent rechargeable batteries, Chem. Soc. Rev., 47 (2018) 7239-7302.
[38] C. Ma, Y. Shu, H. Chen, Preparation of high-purity lead oxide from spent lead paste by low temperature burning and hydrometallurgical processing with ammonium acetate solution, RSC Advances, 6 (2016) 21148-21155.
[39] J. Pan, X. Zhang, Y. Sun, S. Song, W. Li, P. Wan, Preparation of high purity lead oxide from spent lead acid batteries via desulfurization and recrystallization in sodium hydroxide, Ind. Eng. Chem. Res., 55 (2016) 2059-2068.
[40] E. Kim, J. Roosen, L. Horckmans, J. Spooren, K. Broos, K. Binnemans, K.C. Vrancken, M. Quaghebeur, Process development for hydrometallurgical recovery of valuable metals from sulfide-rich residue generated in a secondary lead smelter, Hydrometallurgy, 169 (2017) 589-598.
[41] A. Singh, P. Karandikar, A broad review on desulfation of lead-acid battery for electric hybrid vehicle, Microsyst. Technol., 23 (2017) 2263-2273.
[42] A. Singh, Review on Desulfation of Lead-acid Battery for HEV, Int. Int. J. Curr. Eng. Sci. Res., 2 (2015) 85-96.
[43] Y.X. Zheng, W. Liu, W.Q. Qin, F. Jiao, J.W. Han, K. Yang, H.L. Luo, Reduction of lead sulfate to lead sulfide with carbon monoxide, J. Cent. South Univ., 22 (2015) 2929-2935.

[44] M.A. Kreusch, M.J.J.S. Ponte, H.A. Ponte, N.M.S. Kaminari, C.E.B. Marino, V. Mymrin, Technological improvements in automotive battery recycling, Resour. Conserv. Recy., 52 (2007) 368-380.

[45] C. Huang, C. Tang, M. Tang, J. Yang, Y. Chen, S. Yang, J. He, Sulfur-fixing Reduction Smelting of Spent Lead-acid Battery Colloid Sludge in Fused Salt at Low Temperature, Min. Metall. Eng., 32 (2012) 84-87.

[46] P.B. Queneau, R. Leiby, R. Robinson, Recycling lead and zinc in the United States, World of Metallurgy - ERZMETALL. 68 (2015) 149-162.

[47] W.F. Li, L.H. Jiang, J. Zhan, C.F. Zhang, G. Li, J.Y. Hwang, Thermodynamics Analysis and Industrial Trials of Bottom-Blowing Smelting for Processing Lead Sulfate-Containing Materials, in: 6th International Symposium on High-Temperature Metallurgical Processing, Springer, 2015, pp.507-514.

[48] G. Cusano, M. Gonzalo, F. Farrell, R. Remus, S. Roudier, L. Delgado Sancho, Best Available Techniques (BAT) Reference Document for the main Non-Ferrous Metals Industries, European IPPC Bureau, European Commission, Joint Research Centre, 2017, pp.505-510.

[49] A. Lassin, P. Piantone, A. Burnol, F. Bodénan, L. Chateau, C. Lerouge, C. Crouzet, D. Guyonnet, L. Bailly, Reactivity of waste generated during lead recycling: an integrated study, J. Hazard. Mater., 139 (2007) 430-437.

[50] C. Mohanty, S. Adapala, B. Meikap, Removal of hazardous gaseous pollutants from industrial flue gases by a novel multi-stage fluidized bed desulfurizer, J. Hazard. Mater., 165 (2009) 427-434.

[51] M. Sonmez, R. Kumar, Leaching of waste battery paste components. Part 1: Lead citrate synthesis from PbO and $PbO_2$, Hydrometallurgy, 95 (2009) 53-60.

[52] T. Dutta, K.H. Kim, A. Deep, J.E. Szulejko, K. Vellingiri, S. Kumar, E.E. Kwon, S.-T. Yun, Recovery of nanomaterials from battery and electronic wastes: A new paradigm of environmental waste management, Renew. Sustain. Energ. Rev., 82 (2018) 3694-3704.

[53] D. Andrews, A. Raychaudhuri, C. Frias, Environmentally sound technologies for recycling secondary lead, J. Power Sources, 88 (2000) 124-129.

[54] X. Ma, S. Wang, X. Li, Recycling of lead from the wasted lead-acid battery by solid phase electrolysis, Mater. Res. and Appl., 2 (2008) 141-144.

[55] A. Schröder-Wolthoorn, S. Kuitert, H. Dijkman, J.L. Huisman, Application of sulfate reduction for the biological conversion of anglesite ($PbSO_4$) to galena (PbS), Hydrometallurgy, 94 (2008) 105-109.

[56] J. Weijma, K. de Hoop, W. Bosma, H. Dijkman, Biological conversion of anglesite ($PbSO_4$) and lead waste from spent car batteries to galena (PbS), Biotechnol. Progr., 18 (2002) 770-775.

[57] D. Lin, K. Qiu, Recycling of waste lead storage battery by vacuum methods, Waste Manag., 31 (2011) 1547-1552.

[58] K. Liu, J. Yang, S. Liang, H. Hou, Y. Chen, J. Wang, B. Liu, K. Xiao, J. Hu, J. Wang, An Emission-Free Vacuum Chlorinating Process for

Simultaneous Sulfur Fixation and Lead Recovery from Spent Lead-Acid Batteries, Environ. Sci. Technol., 52 (2018) 2235-2241.
[59] V. Hotea, Clean Technology of Lead Recovery from Spent Lead Paste, Recent Researches in Applied Economics and Management, Econ. Aspects Environ., 2 (2013) 263-270.
[60] Y. Hu, C. Tang, M. Tang, Y. Chen, Extraction of lead from secondary lead through a low-temperature alkaline and sulfur-fixing smelting process, Chin. J. Eng., 37 (2015) 588-594.
[61] Y. Hu, C. Tang, M. Tang, Y. Chen, J. Yang, S. Yang, J. He, Reductive smelting of spent lead-acid battery colloid sludge in molten salt of sodium at low temperature, China Nonferr. Metall., 43 (2014) 75-79.
[62] M. Rämä, S. Nurmi, A. Jokilaakso, L. Klemettinen, P. Taskinen, J. Salminen, Thermal Processing of Jarosite Leach Residue for a Safe Disposable Slag and Valuable Metals Recovery, Metals, 8 (2018) 744-753.
[63] M. Rämä, Experimental investigation of jarosite residue thermal processing, M.Sc. Thesis. Aalto Univ. (2017).
[64] J. Zhang, Y. Yan, Z. Hu, X. Fan, Y. Zheng, Utilization of low-grade pyrite cinder for synthesis of microwave heating ceramics and their microwave deicing performance in dense-graded asphalt mixtures, J. Clean. Prod., 170 (2018) 486-495.
[65] I. Alp, H. Deveci, E. Yazıcı, T. Türk, Y. Süngün, Potential use of pyrite cinders as raw material in cement production: results of industrial scale trial operations, J. Hazard. Mater., 166 (2009) 144-149.
[66] M. Al-harahsheh, J. Al-Nu'airat, A. Al-Otoom, H. Al-jabali, M. Al-zoubi, Treatments of Electric Arc Furnace Dust and Halogenated Plastic Wastes: A Review, J. Environ. Chem. Eng., (2018) 102856-102879.
[67] A. Toghroli, M. Shariati, F. Sajedi, Z. Ibrahim, S. Koting, E.T. Mohamad, M. Khorami, A review on pavement porous concrete using recycled waste materials, Smart Struct. Syst., 22 (2018) 433-440.
[68] L. Ye, C. Tang, Y. Chen, S. Yang, J. Yang, W. Zhang, One-step extraction of antimony from low-grade stibnite in Sodium Carbonate–Sodium Chloride binary molten salt, J. Clean.Prod., 93 (2015) 134-139.
[69] C. Tang, M. Tang, W. Yao, Y. Ruan, J. Peng, Pilot test of reduction-matting smelting of jamesonite concentrate woth short rotary furnace, Min.Metall.Eng., 24 (2004) 51-53.
[70] L. Ye, C. Tang, Y. Chen, S. Yang, M. Tang, The thermal physical properties and stability of the eutectic composition in a $Na_2CO_3$–NaCl binary system, Thermochim. Acta, 596 (2014) 14-20.
[71] B. Toby, CMPR - a powder diffraction toolkit, J. Appl. Crystallogr., 38 (2005) 1040-1041.
[72] Y. Li, S. Yang, P. Taskinen, J. He, F. Liao, R. Zhu, Y. Chen, C. Tang, Y. Wang, A. Jokilaakso, Novel recycling process for lead-acid battery paste without $SO_2$ generation-Reaction mechanism and industrial pilot campaign, J. Clean.Prod., 217 (2019) 162-171.
[73] A. Roine, HSC Chemistry for Windows, vers. 9.2.6, Outotec, Research, Pori, Finland, Outokumpu Research Oy, Pori, Finland, (2017).

[74] M.v., MTDATA ver. 8.2., NPL, Teddington, U.K., 2015. (www.npl.co.uk/sciencetechnology/mathmatics-modelling-and-similation/mtdata/)

[75] J. Gisby, P. Taskinen, J. Pihlasalo, Z. Li, M. Tyrer, J. Pearce, K. Avarmaa, P. Björklund, H. Davies, M. Korpi, S. Martin, L. Pesonen, J. Robinson, MTDATA and the Prediction of Phase Equilibria in Oxide Systems: 30 Years of Industrial Collaboration, Metall. Mater.Trans. B, 48 (2017) 91-98.

[76] Q. Liu, J. Tan, C.Q. Liu, Z.L. Yin, Q.Y. Chen, L. Zhou, F.C. Xie, P.M. Zhang, Thermodynamic study of metal sulfate decomposition process in bath smelting, Chin. J. Nonferr. Metals, 24 (2014) 1629-1636.

[77] Y.X. Zheng, W. Liu, W.Q. Qin, J.W. Han, K. Yang, H.L. Luo, Selective reduction of $PbSO_4$ to PbS with carbon and flotation treatment of synthetic galena, Physicochem. Probl. Miner. Process., 51 (2015)535-546.

[78] Y. Zheng, W. Liu, W. Qin, F. Jiao, J. Han, K. Yang, H. Luo, Reduction of lead sulfate to lead sulfide with carbon monoxide, J. Cent. South Univ., 22 (2015) 2929-2935.

[79] L. Zhan, S. Shen, B. Xie, K. Yang, A novel method of preparing PbS from waste lead paste through in-situ vulcanization and reduction, Journal of Cleaner Production, 208 (2019) 778-784.

[80] Y.J. Hu, C.B. Tang, M.T. Tang, Y.M. Chen, Reductive smelting of spent lead–acid battery colloid sludge in a molten $Na_2CO_3$ salt, International Journal of Minerals, Metallurgy, and Materials, 22 (2015) 798-803.

[81] Y.M. Chen, L.G. Ye, C.B. Tang, S.H. Yang, M.T. Tang, W.H. Zhang, Solubility of Sb in binary $Na_2CO_3$–NaCl molten salt, Trans. Nonferr. Metals Soc. China, 25 (2015) 3146-3151.

[82] L.G. Ye, Y.J. Hu, Z.M. Xia, C.B. Tang, Y.M. Chen, M.T. Tang, Solution behavior of ZnS and ZnO in eutectic $Na_2CO_3$–NaCl molten salt used for Sb smelting, J. Cent. South Univ., 24 (2017) 1269-1274.

[83] Y.M. Chen, Y.E. L. G., C.B. Tang, S.H. Yang, M.T. Tang, W.H. Zhang, Solubility of Sb in binary $Na_2CO_3$–NaCl molten salt, Trans. Nonferr. Metals Soc. China, 25 (2015) 3146-3151.

[84] Y. Li, S. Yang, W. Lin, P. Taskinen, J. He, Y. Wang, J. Shi, Y. Chen, C. Tang, A. Jokilaakso, Cleaner Extraction of Lead from Complex Lead-Containing Wastes by Reductive Sulfur-Fixing Smelting with Low $SO_2$ Emission, Minerals, 9 (2019) 119-124.

[85] Y. Li, Y. Chen, H. Xue, C. Tang, S. Yang, M. Tang, One-Step Extraction of Antimony in Low Temperature from Stibnite Concentrate Using Iron Oxide as Sulfur-Fixing Agent, Metals, 6 (2016) 153-165.

[86] H. Pan, Y. Geng, H. Dong, M. Ali, S. Xiao, Sustainability evaluation of secondary lead production from spent lead acid batteries recycling, Resour., Conserv. Recy., 140 (2019) 13-22.

[87] L. Guangdong Xinsheng Environmental Science & Technology Co., Chaozhou, China, Company profile and technical process, 2014 http://www.xsept.cn/.

Lead-acid batteries are increasingly scrapped in urban areas, especially in the emerging economies, due to their mean lifetime of 2–3 years. LABs are classified as hazardous materials in many countries and their disposal has become a significant environmental concern. Pyrometallugy currently dominates the lead recycling industry worldwide. However, due to the depleting primary resources and increasingly stringent environmental requirements, lead recycling industry is currently under pressure to develop more sustainable processes to achieve new standards of production and emissions. Consequently, researching novel and environment-friendly waste recycling techniques to increase knowledge and enable process optimization for lower environmental impact is mandatory for the modern technology-based society.
The research work presented in this dissertation was conducted under a well-organized double-degree (doctoral) project between Aalto University and Central South University.

Aalto-DD 95/2019

ISBN 978-952-60-8561-6 (printed)
ISBN 978-952-60-8562-3 (pdf)
ISSN 1799-4934 (printed)
ISSN 1799-4942 (pdf)

**Aalto University**
**School of Chemical Engineering**
**Department of Chemical and Metallurgical Engineering**
**www.aalto.fi**

BUSINESS + ECONOMY

ART + DESIGN + ARCHITECTURE

SCIENCE + TECHNOLOGY

CROSSOVER

**DOCTORAL DISSERTATIONS**